VOLUME 23, 1961/62, No. 4 pp. 101-132 Published 25th January 1962

Philips Technical Review

DEALING WITH TECHNICAL PROBLEMS
RELATING TO THE PRODUCTS, PROCESSES AND INVESTIGATIONS OF
THE PHILIPS INDUSTRIES

THE BALANCE OF NATURE

by R. van der VEEN *).

632.95.024

The article below reproduces, with some minor changes, the text of the inaugural lecture delivered by the author on 6th February 1961 as professor extraordinary of botany at the University of Utrecht. The author sketches the "balance of nature" as a state of equilibrium in constant evolution, from primeval forest to single-crop farming, and from the attendant menace of agricultural pests to the present practice of combating these pests with chemical agents. He draws attention to the curious fact that plants themselves use chemical agents in an internecine struggle for existence, and develops the intriguing concept of a "negative biology" based on the action of pesticides, which promises to penetrate far into the secrets of living matter.

The text published here is supplemented, with the kind assistance of the author, by illustrations, a bibliography and an appendix of structural formulae.

Many publications addressed to the general public speak of the "balance of nature". They may often give the impression that this balance is more or less labile, so easily does it seem liable to disturbance. One might imagine that nature is comparable to a chemical balance, so that a slight shift in the balancing forces implied might be expected to "tip the scales" right over.

An equilibrium as achieved on a chemical balance is however never encountered in nature. Darwin [1]) and others have described at considerable length how the balance of nature in fact operates.

The primeval forest

Darwin was one of the first to see the tropical forest not as a community of plants in peaceful coexistence, but on the contrary as the scene of a silent but merciless struggle for food, space and, above all, light. The weapons employed in that struggle are extraordinarily varied. Some plants exploit their physiological aptitude for vigorous upward growth to break out rapidly above the gloom of the lower levels and so offer a broad crown to the light. Other plants are so physiologically adapted as to be able to populate these lower levels (*fig. 1*).

I mention the word physiological because, as a physiologist myself, I think in the first place of such properties as the highly economical photosynthesis required for the formation of enough assimilates at low light intensities; of growth hormones, like auxins and gibberellins, which induce exceptional elongation in many plants; and of factors which, in spite of that elongation, enable the plant to develop a sufficiently sturdy stem.

There are other plants, e.g. lianas, whose excessive elongation prevents them from acquiring the necessary sturdiness, and yet they still contrive to reach the higher levels by climbing up other plants, which may ultimately collapse under their burden.

Others again begin their lives in the light by germinating on an upper branch of a fully-grown tree. Such plants are called *epiphytes*. An epiphyte has to be extremely sparing with the mineral salts available to it, for it cannot in general draw them from the soil. If it is capable of sending out aerial roots, as some species of Ficus do, the roots develop downwards and may ultimately reach the ground and penetrate its surface; a tree is thus produced which, as it were, grows from top to bottom. The aerial roots multiply and become rapidly thicker. The epiphyte gradually proliferates around its "host", and at last destroys it. The "tree strangler", now firmly anchored by the lignification of its original aerial roots, spreads out its crown in the place once occupied by its host.

Although the innumerable seeds that fall to the floor of the forest may well germinate, their chance of survival is remote. The struggle is ceaseless and unrelenting, and only the best adapted and most fortunate can develop to maturity. But I need dwell no further on this fierce competition for survival in the primeval forest; it is a subject with which we have grown sufficiently familiar in the hundred years and more that have elapsed since the appearance of Darwin's brilliant work "On the origin of species".

---

*) N.V. Philips-Duphar, Weesp, Netherlands.

The same fierce struggle as in the primeval forest is fought in practically all plant and animal communities. Here too the balance of nature is quite unlike a chemical succeeds in developing to maturity disturbs the existing pattern of relationships to some extent, for it intrudes itself among the other organisms, often destroying its neighbours, and in so doing changes the order of things. By the very fact of preserving itself, every living being, whether plant or animal, has a considerable influence on its environment, which would certainly have looked different without it. Thus, it can be said that the balance of nature is constantly being disturbed to some extent by each plant and each animal.

Fig. 1. Vegetation in the primeval forest: Ruwenzori massif in the Congo. The photograph was taken in a fairly open spot. The characteristic struggle in which the plants deprive each other of essential sunlight is naturally difficult to represent in a photograph.

Man and the balance of nature

Man too is a part of nature in this context, and to preserve himself is bound to shift the established balance, otherwise there would be no room for him. The early tillers of the soil must have been only balance. Every organism that too well aware of the difficulties which are involved in agriculture, in eradicating the existing plant growth and cultivating useful species. The surrounding vegetation will have constantly fought back to recover its lost ground. Only by dint of hard work, ceaseless weeding and the most intensive cultivation of the soil can they ever have succeeded in raising their plants to maturity. Not for nothing is it written in the old Dutch "Katechismus der Natuur" that God created weeds besides the useful herbs, for had He not done so, the farmers would have grown idle [2]).

Plainly, then, the agricultural population is interfering with the balance of nature in a singularly cruel fashion in felling trees and burning woodland, in ploughing and otherwise mechanically working the land. With the growth of world population this interference is assuming enormous proportions. In more densely populated regions little remains of the original flora and fauna. Even so, the best adapted species have lost nothing of their aggressiveness, and the farmer still has no chance to be idle.

The practice of agriculture requires that large acreages be devoted to the specialized cultivation of individual crops (single-crop farming). As a logical result, adapted species amongst the other organisms, whether weeds, insects, eelworms or moulds, have been able to make large-scale invasions (*figs 2* and *3*).

This brings us to the diseases and pests of agriculture. Since almost every animal and plant has its own peculiar parasites, and every agricultural plague

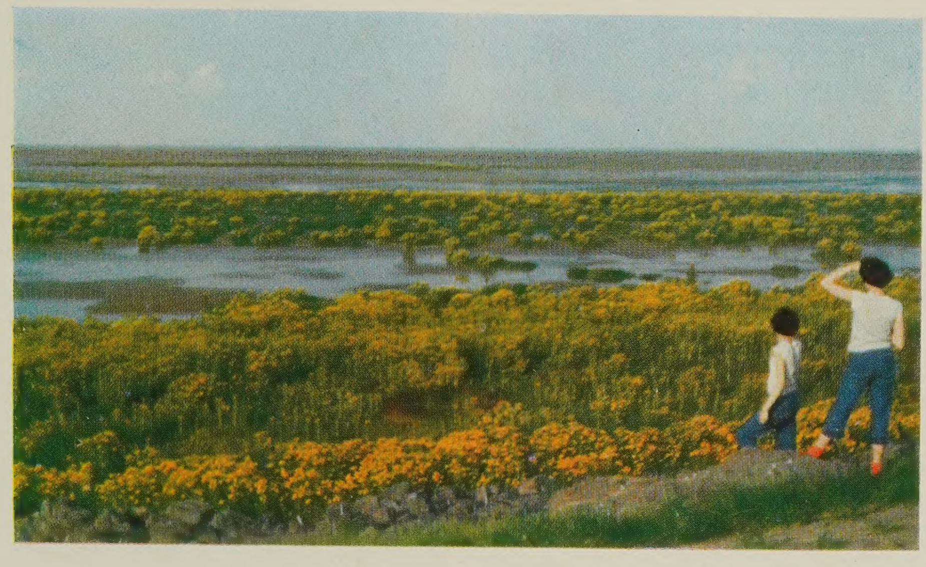

Fig. 2. Land reclaimed from inland seas may often be invaded by adapted weeds. For example, during the drainage of the 140 000-acre Oost-Flevoland polder, formerly a part of the Zuijder Zee, broad expanses were conquered by "marsh endive" (Senecio paluster).

is caused by an animal or plant, pests which flourish in a given cultivated area are always followed by their own parasites.

The demands made on agriculture are steadily growing, and the damage caused by diseases and pests are felt more and more keenly. It is therefore not surprising that the agriculturist must take increasingly drastic measures to derive full benefit from his labour.

People have been so thoroughly accustomed to modern methods of farming, and to the periodic recurrence of pests and diseases, that they regard this state of things as a natural balance. If, for example, after having exterminated large numbers of insects

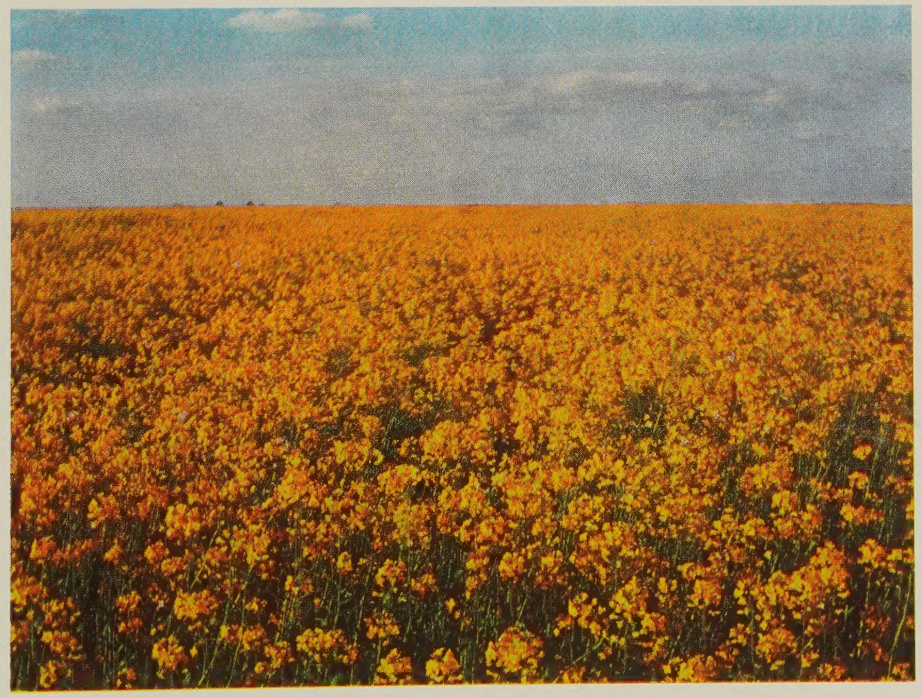

Fig. 3. Another part of the polder shown in fig. 2, in a more advanced stage. The weeds which were formerly present have been replaced by rapeseed. (The 86 000 acres under rapeseed in this polder form the largest area of its kind in Europe.) In the meantime, another pest has developed in this single-crop area: the fields of rapeseed have become thickly infested with weevils.

in his orchards by spraying with DDT [1] *), the fruit-grower finds that his action has enabled the mite population to multiply, he promptly blames himself for having disturbed the balance of nature. Nothing is farther from the truth; that balance was disturbed long ago, and now it has only been shifted a little further.

Usually it is the chemical control agents that are held responsible for such disturbances of the balance of nature. The physical methods, such as felling and burning, tilling, drainage, irrigation and the like, are generally accepted without demur.

It need hardly be said that there are no real grounds whatever for making this distinction between "inhumane chemical" and "humane physical" methods; it springs simply from the mistrust of innovations and the concomitant idealization of the old and familiar.

In fact, nature itself makes widespread use of chemical means of defence and aggression. Many plants, for instance, protect themselves from insects by toxic alkaloids. I need only mention the upas tree of South-East Asia (Antiaris toxicaria), whose milky sap is used as arrow poison.

Another mode of chemical warfare, this time between plants among themselves, takes place below ground. The roots of some plants excrete substances which, if absorbed by the roots of other plants, severely damage the latter or inhibit their growth.

This form of root competition is much more common than might be supposed. Many think of root competition as a struggle for mineral salts or water. That is by no means always the case. Bonner discovered that the rubber-producing guayule plant secretes cinnamic acid [2] from its roots, which acts as a growth-hormone antagonist when taken up by other plants and so inhibits their development ³). In Java we were able to isolate from the soil in which Salvia occidentalis was growing a substance capable of almost completely inhibiting the growth of young coffee plants ⁴) (*fig. 4*).

It was reported some years ago that when land badly infested by eelworms is planted with African marigolds (Tagetes), the eelworm population rapidly declines. This observation attracted considerabbe attention because of the difficulty of controlling this pest effectively. Investigations by Uhlenbroek and Bijlo showed that the roots of Tagetes contain a substance, terthienyl [3], which is extremely toxic to eelworms ⁵). These are just a few of the many indications that the underground struggle in nature is fought, at least in part, by chemical means.

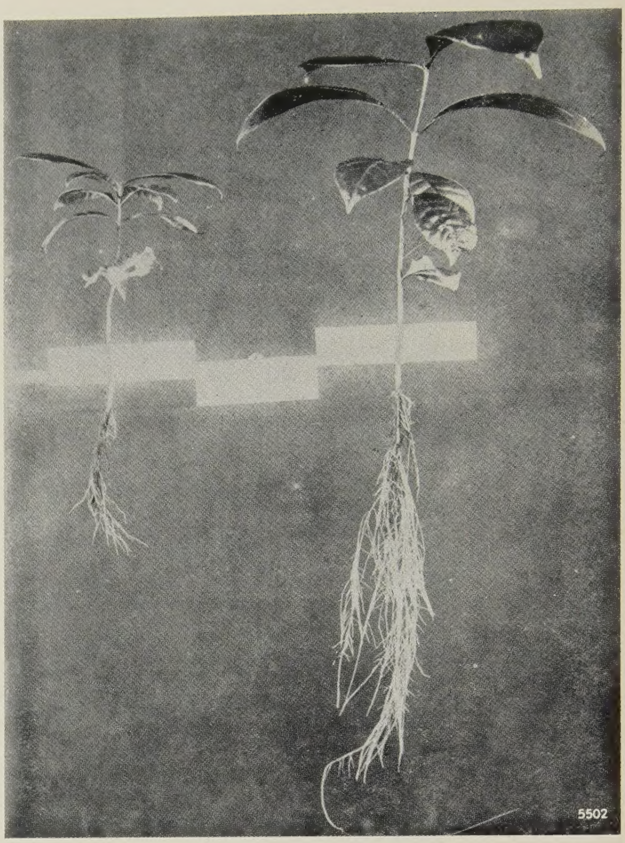

Fig. 4. Example of root competition. The coffee plant on the left was grown together with Salvia occidentalis in a water culture (after which the Salvia was removed). The coffee plant on the right was grown without Salvia. The growth of the left-hand specimen has been severely inhibited by substances excreted from the Salvia roots.

Above the ground, too, nature makes frequent use of chemical agents. One example is the shrub Encelia which has been studied by Went ⁶) and Bonner ³). This plant, a native of the Californian desert, exudes from its leaves a chemical substance that inhibits the germination of seeds. The sporadic rainfall in these arid regions washes the substance on to the ground under the shrubs. The seeds lying there would normally germinate in these humid intervals, but the inhibitor washed from the leaves prevents them from doing so. In this way the Encelia wards off the competition of other plants that might otherwise overwhelm it.

Chemical control of pests, a necessary measure

To control the spontaneous spread of weeds, the chemical industry has developed numerous herbicides which, administered in very small quantities, apparently block an essential biochemical reaction in plants.

Natural vegetation, already so impoverished by mechanical methods of agriculture, is menaced even more by these chemical agents. The botanist, of course, views this development with regret. It is appalling to imagine what the Alpine meadows would look like if weed control of this kind were rigorously applied there. Our own native pastures have lost much of their former beauty now that they are no longer bright with buttercups, ladysmock, dandelions and sorrel, not to mention the wild orchid and other plants now rarely to be found.

---

*) The figures between square brackets refer to the structural formulae in the appendix.

We feel this as a sad deprivation and forget that the severest impoverishment was caused long ago by the growth of the population, resulting in the destruction of forests and the introduction of mechanical methods of cultivation. Chemical methods are simply a further step forward in a development that was initiated by our distant forebears, a development which is making the creation of nature reserves more and more urgently necessary.

Our most sensible policy is undoubtedly to take a realistic view of these chemical innovations in agriculture, and to set bounds to their application by establishing reserves where their use is forbidden. This whole course of events when all is said and done is the consequence of the enormous expansion of world population, which is a much more disquieting phenomenon.

Biochemical equilibria in cells

Before dealing with these pesticides any further, I should like to look for a moment at the structure of living matter, at the organism itself. There is a natural balance in an organism too, but of quite a different kind. Here it is a complex interplay of biochemical processes in which the chemical reactions are on the whole reversible. Each reaction thus represents a state of dynamic equilibrium. If the product of a reaction is removed by a subsequent reaction, the first reaction will continue to proceed in the same direction. If the reaction product accumulates, however, the reaction will come to a standstill or may even be reversed.

Nearly every compound formed in an organism should be seen as a link in a long chain which, with the uptake of energy, can lead to more intricate compounds, or which, upon the dissipation of energy, is normally degraded to simpler compounds.

The picture of a compound as a link in a long chain is really oversimplified. In fact we should think of it as a node in a network, indeed in a three-dimensional network. A system built up in this way can clearly be a stable one. Again, many vital processes are stabilized by ingenious feedback mechanisms. If a line is disturbed anywhere, the process usually continues by a roundabout route. Only the blockage of the most essential lines results in the death of the organism. Now what are these essential lines?

Indications in this direction may well be provided by the multifarious herbicides, fungicides and insecticides in use, for it is precisely these substances, applied in such extremely small concentrations, that yield such remarkable results, albeit in terms of the destruction of living matter. The study of these agents thus constitutes a sort of "negative biology". The following example will serve to illustrate the value of this negative biology in the fields of physiology and biochemistry.

A line of major importance is that along which energy is supplied in living matter. The energy required for synthesis is derived in most cases from the compound adenosine triphosphate [4], generally abbreviated to ATP. This compound is formed in processes of photosynthesis (photosynthetic phosphorylation), respiration (oxidative phosphorylation) and fermentation [7]).

In all three processes the energy made available by the oxidation of reduced compounds is stored in a phosphate bond of the ATP, which can then supply the energy for further processes that need it.

Any substance that impedes the formation of ATP must therefore be highly toxic to the organism. In agriculture substances of this kind are used which inhibit ATP formation in the process of oxidative phosphorylation. Known as "uncouplers", these agents do not stop respiration — on the contrary, they speed it up considerably — but no ATP is produced. The dinitrophenols are powerful uncouplers, and are used in large quantities as herbicides and insecticides (DNBP, DNOC [5]).

The dinitrophenols are also used as respiration uncouplers in many scientific investigations. Processes requiring energy are stopped by such a substance, as the necessary energy is normally supplied to the process via the ATP. In this way it is possible to distinguish energy-consuming processes from those that proceed freely. The dinitrophenols have been used for many years in physiological and biochemical research on e.g. the uptake and translocation of substances in plants. A good deal has thus come to be known about their action.

Another weed killer well known to agriculturists, 2,4-dichlorophenoxyacetic acid [6], belongs to the group of growth substances, its action on the plant being analogous to that of the normal growth hormone, indoleacetic acid [7]. Whereas, however, indoleacetic acid is a link in a chain of enzymatic reactions and is therefore dependent on other reactions both for its synthesis and for its breakdown, the dichlorophenoxyacetic acids do not fit into the biochemical scheme of the plant. They are assimilated and function as if they were growth hormones, but they cannot be broken down in the normal cycle and as a result the growth and development of the plant are completely disorganized (*fig.* 5).

There are some other chemical agents I should now like to mention because of their potential value to fundamental scientific research. Indeed, through their apparent ability to disturb the biological balance inside the cell, they may well provide us with the key to the essential processes in living matter. Unfortunately I must add at once that in this respect they have received far too little attention. What is at present known of their physiological and biochemical action stems mainly from the laboratories of the industries that produce them.

Years after the introduction of chlorophenyldimethyl urea [8], called "Monuron", as a herbicide in agriculture, nothing was known about the mechanism of its action. Wessels concluded on theoretical grounds that it was probably a potent inhibitor of photosynthesis [8]). This in fact proved to be the case, further research showing it to be one of the most active of such substances. So specific an inhibitor will undoubtedly be of considerable value to research into the process of photosynthesis.

Then there are the substituted triazines which, under the names of "Simazin" [9] and "Atrazin", are used in large quantities as weed-killers. It is known that these also inhibit photosynthesis, but it is quite likely that they arrest other vital processes too.

These are just some examples of substances about whose active mechanism we have at least some indications. But there are numerous other herbicides whose active mechanism is still completely unknown. One such substance is the germination inhibitor 2,6-dichlorobenzonitrile [10], minute doses of which make it impossible for most seeds to germinate, and moreover completely stop the growth of young plants (*fig. 6*). Others in this category are marketed under the proprietary names "IPC", "Avadex", "Dalapon", "Amitrol" and "Karsil". Further, there is "Reglone", a bromodipyridyl compound, extremely small concentrations of which (less than 1 pound per acre) are sufficient, in some way still unknown, to derange the physiological balance in plants so thoroughly that they die off in a very short time. It would be highly interesting to discover the particular system on which such minute quantities act.

Amongst the many fungicides in agricultural use, the only ones whose active mechanism is not completely unknown are the dithiocarbaminates [11]. Their physiological action has been elucidated, at least in part, by Kaars Sijpesteyn and co-workers [9]), who also found the explanation for the double peaks in the curves showing the relation between effect and concentration (*fig.* 7).

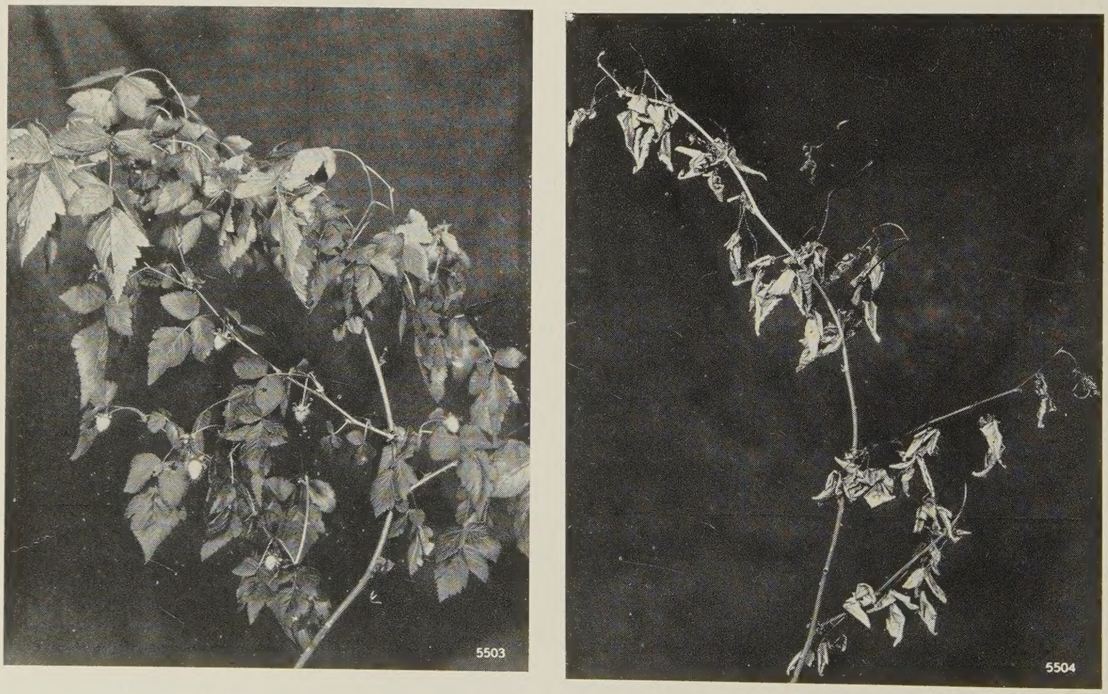

Fig. 5. The effect of the herbicide 2,4,5-trichlorophenoxyacetic acid on brambles is seen from the treated shrub on the right. (The shrub on the left is untreated.) This herbicide acts as a growth hormone, but does not fit into the biochemical scheme of the plant, and therefore completely disorganizes its development.

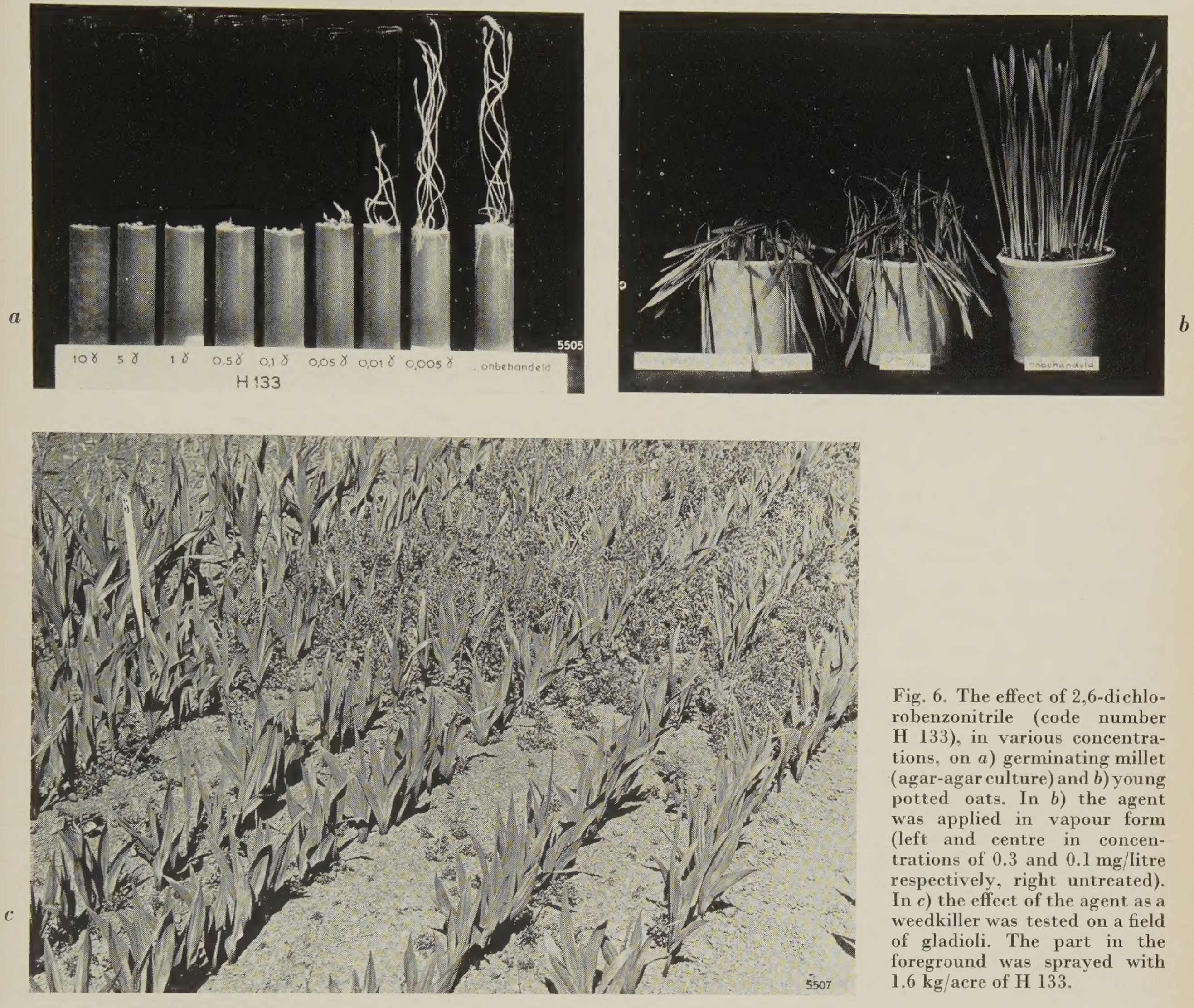

Fig. 6. The effect of 2,6-dichlorobenzonitrile (code number H 133), in various concentrations, on *a*) germinating millet (agar-agar culture) and *b*) young potted oats. In *b*) the agent was applied in vapour form (left and centre in concentrations of 0.3 and 0.1 mg/litre respectively, right untreated). In *c*) the effect of the agent as a weedkiller was tested on a field of gladioli. The part in the foreground was sprayed with 1.6 kg/acre of H 133.

Of the insecticides the group of phosphorus compounds is the subject of a great deal of biochemical research, owing to the fact that they inhibit the enzyme choline-esterase. Since the latter is essential to the proper functioning of the nervous system, the medical profession is keenly interested and various medicophysiological and biochemical laboratories are at present studying these substances.

Apart from this group, there are many more insecticides and acaricides which have so far only been studied as regards their practical application.

Conclusion

It is my opinion that there are many chemical agents used in agriculture that are certainly worth intensive and fundamental research to discover

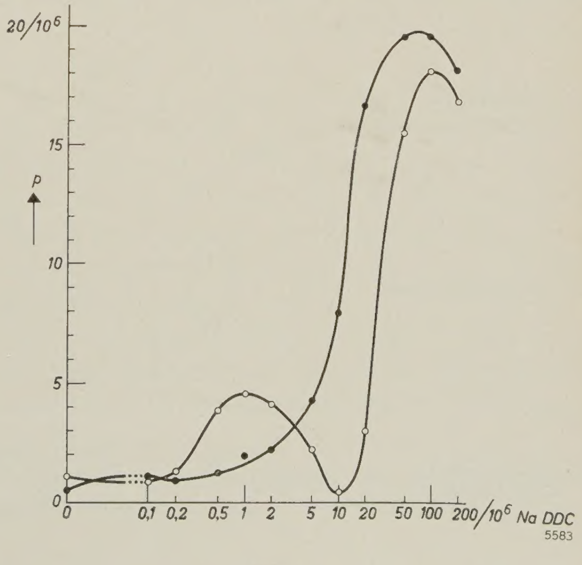

Fig. 7. Example of complications in the action of chemical control agents. The curves show the relation between the concentration of NaDDC [11] and its effect on Aspergillus niger in the presence and absence of copper (white and black circles, respectively). Where copper is present, the curves show two peaks. An explanation of this phenomenon will be found in reference [9]). The ordinate gives the content *p* of accumulated pyruvic acid, which is a measure of the biochemical disturbance on which the action of this pesticide depends.

the mechanism of their action. Some of these substances are already subjects of such research. It is to be hoped that many of the others will soon be subjected to a similar investigation. The best way to make research along these lines yield rich fruit — apart from properly equipping the laboratories in question — is close cooperation between biologists on the one hand and biochemists and agriculturists on the other.

Appendix: structural formulae of some compounds mentioned in the text

[1] DDT . . . .

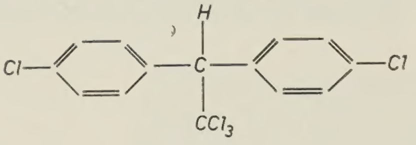

[2] Cinnamic acid . . . .

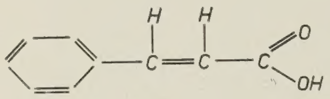

[3] Terthienyl. . . . . .

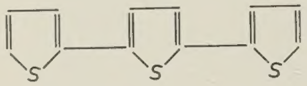

[4] Adenosine triphosphate (ATP). . . . .

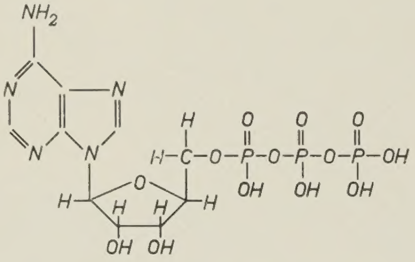

[5] DNOC. . . . .

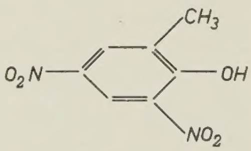

[6] 2,4-Dichlorophenoxyacetic acid

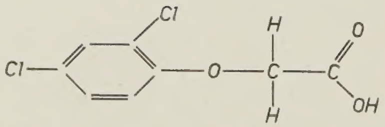

[7] 3-Indoleacetic acid . . . .

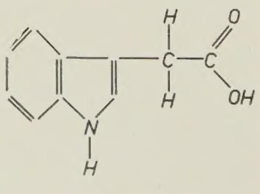

[8] Chlorophenyl-dimethyl urea . . .

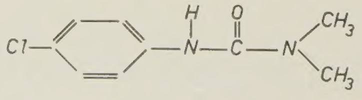

[9] 1-Cl-3,5-diethyl triazine . . . . .

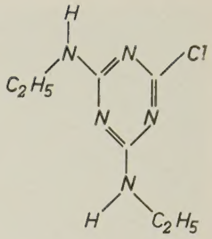

[10] 2,6-Dichlorobenzonitrile . . . .

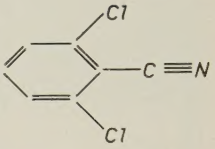

[11] Sodium dimethyl dithiocarbaminate (NaDDC) . . .

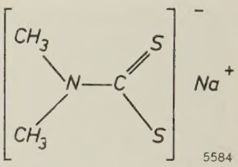

BIBLIOGRAPHY

1) C. R. Darwin, On the origin of species by means of natural selection, 1859.

2) J. F. Martinet, Katechismus der Natuur, published by J. Allart, Amsterdam 1778.

3) J. Bonner, The role of toxic substances in the interactions of higher plants, Bot. Rev. **16**, 51-65, 1950.

4) R. van der Veen, Wortelconcurrentie in de koffie- en rubbertuinen, Archief koffiecult. **9**, 65-102, 1935.

5) J. H. Uhlenbroek and J. D. Bijloo, Proc. 4th int. Congr. crop protection, Hamburg 1957, Part I, 579-581, 1959.

6) F. W. Went, The dependence of certain annual plants on shrubs in Southern California deserts, Bull. Torrey Bot. Club **69**, 100-114, 1942.

7) See e.g. R. van der Veen, De weg van de energie bij levende organismen, Vakbl. Biol. **39**, 173-181, 1959.

8) R. van der Veen and J. S. C. Wessels, Biochim. biophys. Acta **19**, 548, 1956.

9) A. Kaars Sijpesteyn, M. J. Janssen and G. J. M. van der Kerk, Biochim. biophys. Acta **23**, 550, 1957.

For information on the subjects discussed, reference may also be made to the following articles that have appeared in this journal:

R. van der Veen, Influence of light upon plants, Philips tech. Rev. **11**, 43-49, 1949/50.

R. van der Veen, Photosynthesis, ibid. **14**, 298-303, 1952/53.

R. van der Veen, "Boekesteyn", the agrobiological laboratory of N.V. Philips-Roxane, ibid. **16**, 353-359, 1954/55.

J. Meltzer, Research on the control of animal pests, ibid. **17**, 146-152, 1955/56.

M. J. Koopmans, Fungicide research, ibid., pp. 222-229.

R. van der Veen, Growth substances in plants, ibid., pp. 294-298.

W. Duyfjes, The formulation of pesticides, ibid. **19**, 165-176, 1957/58.

Summary. Principal contents of the inaugural lecture delivered by the author as professor extraordinary of botany at the University of Utrecht. In e.g. cultivating the land, man participates in the constant evolution of the "balance of nature". The chemical agents used to this end should not be seen merely as a means of pest control; they can also be of value to the fundamental study of living matter. Their action relies on the disturbance of essential processes in the living organism, and because of that fact they may well be the key to understanding those processes. The author advocates close cooperation between biologists, biochemists and agriculturists with a view to more intensive research into this "negative biology", and mentions various chemical agents that might be studied along these lines.

THE APPLICATION OF CONTROL THEORY TO LINEAR CONTROL SYSTEMS

by M. van TOL *).

621-53.001

Up to the beginning of the 'forties, control engineering was approached largely on an empirical basis; measures taken to improve a control system tended to rely more on practical experience and intuition than on theoretical insight. Improvement came when it was recognized that the theory of control systems and servomechanisms could be derived directly from the theory of negative-feedback amplifiers.

The article below discusses the present-day treatment of control problems with the aid of complex variables, a method commonly used in alternating-current theory. As one example, an analysis is given of the frequency response characteristics of the temperature-control system used in the subcritical suspension reactor at Arnhem (Netherlands), previously described in this journal.

Introduction

Equipping a plant with a system for automatically controlling a variable such as temperature, liquid level or gas flow amounts essentially to giving it negative feedback and amplification. The output signal Θ_o of the instrument that measures the variable is compared with a reference (input) signal Θ_i, and their difference ε is amplified and used to control the regulating device (*fig. 1*). It is therefore not surprising that control theory runs parallel with the theory of negative-feedback amplifiers and network analysis, developed in the 'twenties for the purposes of electronic engineering [1]).

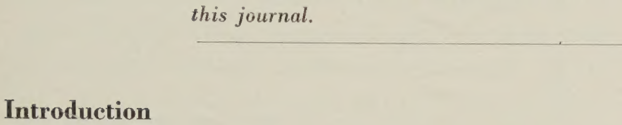

Fig. 1. Block diagram of an automatic control system. *I* plant. *II* instrument which measures the quantity to be controlled. The output signal Θ_o from *II* is compared in *III* with the reference signal Θ_i. The difference ε between Θ_o and Θ_i is the input signal of the controlling unit *IV*, the output signal of which controls the regulating unit *V*. The latter in turn acts directly on the quantity to be kept constant.

An analysis of the characteristics of an automatic control system is concerned with the closed loop (cf. fig. 1) formed by the plant in which the process to be controlled takes place, the measuring unit, the controlling unit, and the regulating unit. If all the elements composing the control loop are *linear*, the problem can be treated exactly with the aid of *complex variables*. Other methods will not be considered here.

When applying this method to the analysis of a negative-feedback amplifier, the starting point is to take the characteristics of the amplifier *without* feedback. The same procedure is applied to a control system. The loop is regarded as opened at some point — e.g. at the dotted line in fig. 1 — and an *open-loop transfer function* is assigned to it. This function, as in AC theory, is the ratio of the complex quantities which can be formed from a sinusoidal input and output signal — both having an angular frequency ω — by replacing the trigonometric function by an exponential function with an imaginary exponent. The symbols Θ_i and Θ_o used above for the input and output signals in fact denote these complex quantities.

The transfer function is normally split into a constant real factor K and a complex variable $G(j\omega)$. The latter describes the variation with ω both of the gain (amplitude response) and of the phase shift φ between input and output signals. Since all elements of the loop are assumed to be linear, KG is equal to the product of the transfer functions K_1G_1, K_2G_2, etc. of the individual elements. It is therefore immaterial where the loop is imagined to be opened.

In this article we shall consider three examples of the way in which a transfer function is found in practice from an analysis of the physical data of a given process. The first example relates to controlling the level in a tank, a problem frequently encountered in the chemical industry; the second concerns the control of temperature in a glass-furnace feeder which was recently described in this journal [2]), and the third the system of controlling the suspension temperature in the subcritical nuclear reactor at the

---

*) Research Laboratories, Eindhoven.

[1]) This theory will be found in e.g. H. W. Bode, Network analysis and feedback amplifier design, Van Nostrand, New York 1945.

[2]) See P. M. Cupido, Philips tech. Rev. 22, 311-319, 1960/61 (No. 9/10).

N.V. KEMA laboratories in Arnhem, also recently described in this journal[3]). It will be seen that the physical analysis referred to must often rely on approximations.

For the convenience of readers unfamiliar with the subject, we shall first examine the KG function at somewhat greater length in order to show how fundamental it is to control theory.

The transfer function

The importance of the KG function in control theory becomes immediately evident when we try to answer the following two questions: how far does the control system reduce a disturbance Θ_s, and is the closed loop sufficiently stable? We will first consider the case where the disturbance can only occur behind the last block in fig. 1. The control loop can then be reduced to the diagram in *fig. 2*. In that case

$$\Theta_o = KG\varepsilon + \Theta_s, \quad . \; . \; . \; . \; . \quad (1)$$

or, since $\varepsilon = \Theta_i - \Theta_o$,

$$(1 + KG)\Theta_o = KG\Theta_i + \Theta_s,$$

hence

$$\Theta_o = \frac{KG}{1 + KG}\Theta_i + \frac{1}{1 + KG}\Theta_s. \quad . \quad (2)$$

If we only want to know the extent to which a sinusoidal disturbance is suppressed, we may put $\Theta_i = 0$, giving

$$\frac{\Theta_o}{\Theta_s} = \frac{1}{1 + KG}. \quad . \; . \; . \; . \; . \; . \quad (3)$$

The absolute value of this ratio is called the *deviation ratio*[4]).

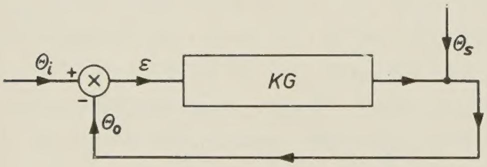

Fig. 2. Block diagram of control loop in which the disturbance Θ_s can only occur behind the last unit (cf. fig. 1).

It will thus be clear that the effect of the disturbance is not eliminated, but reduced by the factor given in eq. (3). The remaining effect is called the *deviation*. (In theory a zero deviation can be achieved by inserting an integrator in the loop, for which element G approaches infinity as ω approaches zero.)

As regards the *stability* of the system the magnitude of Θ_s is unimportant, and (2) reduces to

$$\frac{\Theta_o}{\Theta_i} = \frac{KG}{1 + KG}. \quad . \; . \; . \; . \; . \; . \quad (4)$$

The significance of this equation will be made clear presently.

We now turn to the case where the disturbance occurs not at the end of the loop but at a point somewhere in the middle (*fig. 3*). We represent the transfer function of the blocks in front of that point by K_1G_1, that of the others by K_2G_2. Writing $K_1G_1K_2G_2$ as KG, the output signal in this case is

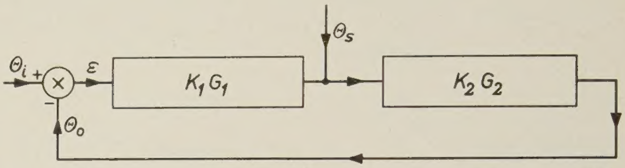

Fig. 3. Control loop where the disturbance signal Θ_s occurs somewhere in the middle. The transfer function of the units in front of this point is K_1G_1, that of the others K_2G_2.

$$\Theta_o = KG\varepsilon + K_2G_2\,\Theta_s, \quad . \; . \; . \quad (5)$$

which, in the same way as above, leads to

$$\Theta_o = \frac{KG}{1 + KG}\Theta_i + \frac{K_2G_2}{1 + KG}\Theta_s. \quad . \quad (6)$$

From this relationship we again first derive the deviation ratio, i.e. the quotient of the values of the output signal with and without control action for the case where $\Theta_i = 0$. We find

$$\frac{\Theta_o}{\Theta_s K_2G_2} = \frac{1}{1 + KG}. \quad . \; . \; . \; . \quad (7)$$

For the stability of the system we again assume $\Theta_s = 0$ in equation (6), which once more yields

$$\frac{\Theta_o}{\Theta_i} = \frac{KG}{1 + KG}. \quad . \; . \; . \; . \; . \; . \quad (8)$$

Apart from the fact, which is trivial, that equations (4) and (8) are identical, we see that the right-hand side of eq. (7) is identical with that of (3). *The general rule is that to analyse both the stability of the system and the factor by which disturbances are reduced it is necessary to have the transfer function of the whole assemblage of units in series, i.e. the KG function of the open loop.*

The behaviour of an open control loop can also be represented graphically, either by a polar plot of the KG function in the complex plane (Nyquist diagram) or by first deriving from KG the separate amplitude and phase characteristics and plotting these in some convenient way. The Nyquist diagram is useful for finding quickly the absolute value P of the function $1 + KG$ at a particular frequency. This is done by joining the relevant point on the curve to the point (—1,0) on the axis, as illustrated in *fig. 4*.

---

[3]) See B. L. A. van der Schee and M. van Tol, Philips tech. Rev. **21**, 121-133, 1959/60.

[4]) J. M. L. Janssen, Trans. Amer. Soc. Mech. Engrs. (ASME) **76**, 1303, 1954.

The frequency response curves are often plotted on a logarithmic scale: the amplitude characteristic in logarithmic coordinates and the phase characteristic in semilogarithmic coordinates (Bode diagram). This method offers advantages when the maximum permissible gain is to be determined.

As far as *stability* is concerned it will be sufficient here to note that the frequency response curves should be such that the gain $|KG(j\omega)|$ is less than unity at the frequency ω_c where φ is —180°, i.e. where the negative feedback in the loop has changed to positive feedback (regeneration). In the Nyquist diagram this means that the curve must not enclose the point (—1,0) [5].

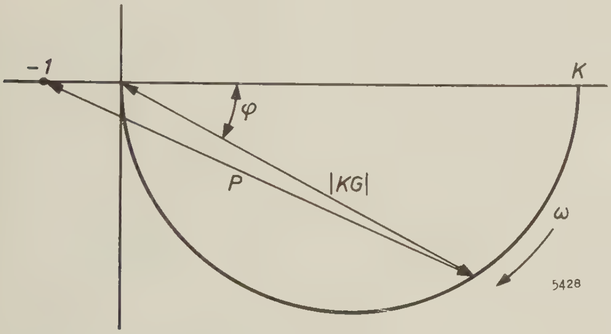

Fig. 4. Nyquist diagram of the function $KG = K(1 + j\omega\tau)^{-1}$. The distance from a point on the curve to the origin gives the absolute value of KG at the relevant frequency, i.e. the gain. Disturbances are reduced by the factor P, found from the distance of a point on the curve to the point $(-1,0)$. The phase shift φ between output and input signal runs here from 0 to $-90°$.

In addition to Bode and Nyquist diagrams the graphical methods shown in *fig. 5* are sometimes used. The plot in fig. 5*a*, called a Nichols chart, is in effect a Nyquist diagram drawn in semilogarithmic rectangular coordinates. In fig. 5*b*, called the inverse Nyquist diagram, the reciprocal of KG is drawn in the complex plane. This method is useful for quickly determining the response of the closed loop, since it follows from (4) that $\Theta_i/\Theta_o = (1 + KG)/KG = KG^{-1} + 1$.

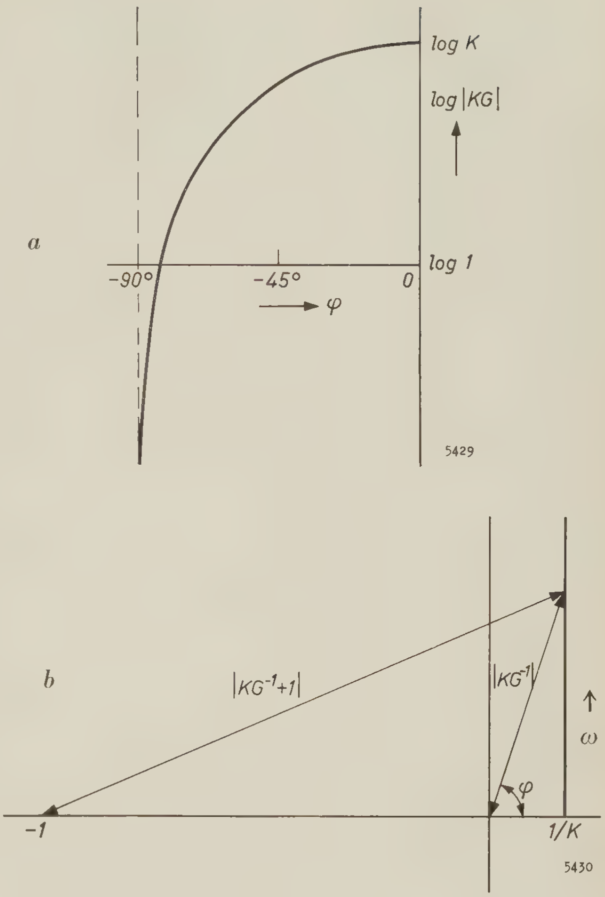

Fig. 5. *a*) Relation between log $|KG|$ and φ for the transfer function $KG = K(1 + j\omega\tau)^{-1}$ (cf. fig. 4) plotted in rectangular coordinates (Nichols chart).
b) Graph of the function $1/KG$ in the complex plane, likewise for the case $KG = K(1 + j\omega\tau)^{-1}$.

Example of the determination of the transfer function of a single element

As an example of the method used to determine the transfer function of an element we take an open tank into which water is run from a tap (rate of flow I_1) and at the same time run off through an outlet (rate of flow I_2). The tank is assumed to be of uniform width, area of base F, so that the volume of water V in the tank is proportional to the height H to which the tank is filled (*fig. 6*). It is further assumed that I_2 is proportional to H, which we may write $I_2 = c \times H$. If I_1 is constant (value I_0),

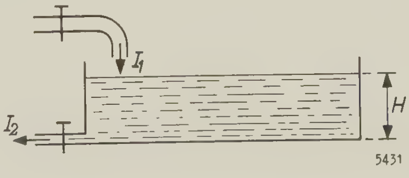

Fig. 6. For calculating the transfer function of a tank filled with water from a tap (flow rate I_1, independent variable) and emptied through an outlet where the flow rate I_2 is proportional to the height H.

---

[5] For complicated control systems the stability criterion as formulated here is oversimplified, but it is adequate for the relatively simple systems discussed in this article. The stability problem is dealt with at some length e.g. by G. S. Brown and D. P. Campbell, Principles of servomechanisms, Wiley, New York 1948, and by G. J. Thaler and R. G. Brown, Servomechanism analysis, McGraw-Hill, New York 1953.
The relation between stability and gain will be dealt with in the next number of this journal.

the value H_0 which H has in the steady state is such that I_2 is equal to I_0, and therefore $H_0 = I_0/c$. We now want to ascertain how H will fluctuate around the value H_0 when I_1 is not constant but shows a sinusoidal ripple of amplitude $\hat{i}_1$ and angular frequency ω:

$$I_1 = I_0 + i_1 \sin \omega t.$$

The problem is defined by the differential equation

$$I_1 - I_2 = \frac{\mathrm{d}V}{\mathrm{d}t} = F\frac{\mathrm{d}H}{\mathrm{d}t},$$

or, substituting $H_0 + h$ for H and given $I_0 = cH_0$,

$$F\frac{\mathrm{d}h}{\mathrm{d}t} + c\,h = \hat{i}_1 \sin \omega t\,. \quad . \quad . \quad (9)$$

We can readily solve an equation of this kind by finding a solution of the form $\bar{h} = \hat{h}\,\mathrm{e}^{\mathrm{j}\omega t}$ for the equation

$$F\frac{\mathrm{d}\bar{h}}{\mathrm{d}t} + c\,\bar{h} = \bar{i}_1\,, \quad . \quad . \quad . \quad . \quad (10)$$

where $\bar{i}_1 = \hat{i}_1\,\mathrm{e}^{\mathrm{j}\omega t}$. Substituting the expression for $\bar{h}$ in eq. (10), we obtain

$$F\,\mathrm{j}\omega\bar{h} + c\,\bar{h} = \bar{i}_1\,,$$

or

$$\bar{h} = \frac{\bar{i}_1}{F\mathrm{j}\omega + c} = \frac{\bar{i}_1/c}{1 + \mathrm{j}\omega\tau}, \quad . \quad . \quad (11)$$

where τ represents the quotient F/c, which is easily seen to have the dimension of time. Since finding the KG function consists in finding the ratio of the complex quantities corresponding to the input and output signals, it follows from equation (11) that

$$KG = \frac{1/c}{1 + \mathrm{j}\omega\tau},$$

whence

$$K = 1/c \quad \text{and} \quad G = \frac{1}{1 + \mathrm{j}\omega\tau}. \quad . \quad (12)$$

(The factor $1/c$ in the numerator of (11) is not a gain factor but a dimensional factor, due to our choice of h as the starting quantity instead of the flow I_2. If we had started with I_2, K would have been unity; there is no amplification of the input signal.)

The form of the G function found here is frequently encountered in practice. The operation of most circuit elements used in control systems can be defined by an arrangement of blocks in series — as many blocks as there are time constants — having a transfer function of the form $K(1 + \mathrm{j}\omega\tau)^{-1}$. Some familiar electrical circuits that have this transfer function are shown in *Table I*. The last one may be regarded as the equivalent electrical circuit of the tank in our example.

Table I. Electrical circuits whose transfer function can be expressed in the form $K(1 + \mathrm{j}\omega\tau)^{-1}$. In the third example the input and output quantities have different dimensions, resulting in a dimensional factor R. The gain factor is in each case equal to unity.

Circuit	Input and output quantities	Transfer function	τ
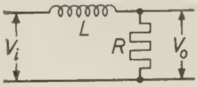	V_i, V_o	$\dfrac{R}{R+\mathrm{j}\omega L} = \dfrac{1}{1+\mathrm{j}\omega L/R}$	L/R
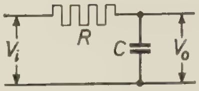	V_i, V_o	$\dfrac{1/\mathrm{j}\omega C}{1/\mathrm{j}\omega C+R} = \dfrac{1}{1+\mathrm{j}\omega RC}$	RC
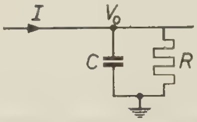	I, V_o	$\dfrac{1}{1/R+\mathrm{j}\omega C} = R\dfrac{1}{1+\mathrm{j}\omega RC}$	RC

Control of the glass temperature in a tank-furnace feeder

As our second example we shall consider a system for controlling the temperature of molten glass in the feeder from a tank furnace to a glass-working machine. In the article cited [2]) it was explained that it is important to ensure that the conditions under which glass is produced are kept as uniform as possible. The first prerequisite is to keep the temperature of the glass in the melting tank carefully constant. Since this cannot be done directly, the various quantities which affect the glass temperature are stabilized separately. These quantities are the temperature of the fuel oil for the burners, the pressure of the atomizing air, the flow rates of oil and air to the burners (or possibly the flow rate of the air and the ratio of oil flow to air flow), the pressure of the combustion gases above the glass, and the level in the tank. From the melting tank the glass flows through the "working end" of the furnace into one or more feeders for the glass-working machines. Since the flow of glass to the machines must be constant, the temperature in the feeder is separately controlled; this control must be very rigorous, because the viscosity of the glass, which has a great effect on its rate of flow, is highly temperature-dependent. We shall now examine the control system used for this purpose.

The temperature of the glass in the feeder is controlled with the aid of an electrical thermometer, which is immersed in the molten glass and whose output signal is used to regulate the burners — gas burners in this case (*fig.* 7); we shall not discuss the practical details of this control here. A block diagram of the control system is shown in *fig. 8*. Block *I* is the feeder with molten glass, which receives a specific flow of heat and acquires the temperature Θ_t. Block *II* is the thermometer, whose output signal Θ_o is compared with the desired value Θ_i. The difference ε is amplified in block *III* — we assume provisionally that the amplification A is linear and independent of frequency. The output from *III* controls the valve *IV* which regulates the gas supply and thus indirectly the flow of heat to the gas. Let us now try to find the transfer function of this system.

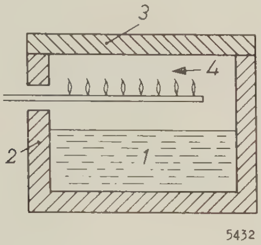

Fig. 7. Heating of molten glass in a glass-furnace feeder. *1* glass, *2* wall of feeder. *3* roof. *4* gas burner

We shall argue presently that the feeder with molten glass, like the water tank discussed, behaves in principle like the electrical circuit of a resistance and capacitance in parallel (see example 3 in Table I). The current I represents the flow of heat from the burners to the glass, the capacitance C the heat capacity of the glass, R the thermal resistance over which the heat is dissipated, and V_0 the temperature to be kept constant. Disturbances that arise may be due to fluctuations in I, C or R. Fluctuations in C may be due to variations in the level of glass, fluctuations in R to variations in the chimney draught. We shall confine ourselves here to variations in I. Putting $RC = \tau_I$, the frequency-dependent part of the transfer function for block I is given by

$$G_I = \frac{1}{1 + j\omega\tau_I}. \quad \ldots\ldots \quad (13)$$

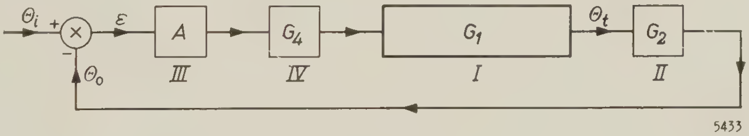

Fig. 8. Block diagram (simplified) of system for controlling the temperature of the molten glass flowing through a feeder from the glass furnace to the glass-working machine. *I* feeder. *II* thermometer. *III* linear amplifier. *IV* regulating valve.

Because of the very high values assumed by the heat capacity of the glass and the thermal resistance, τ_I is of the order of magnitude of half an hour.

In order to justify the assumption that this case may in fact be identified, as a first approximation, with the third example in Table I, we shall look at what happens in the feeder (see fig. 7). The heat delivered by the burners is partly transferred to the glass and partly to the walls and roof of the feeder. The ratio between the two heat flows will be roughly independent of the magnitude of the total heat flow. The way in which the heat is transported from the flame to the glass need not be considered here. All we are interested in is the fact that there is a flow of heat to the glass that depends on the flow of gas to the burners, and which responds almost without any lag to a change in the gas flow.

It remains to be shown that the process of heat removal may be regarded as the flow of current through a resistance as a result of a potential difference V_0 which represents the temperature difference ΔT between the glass and the surroundings of the furnace. The heat is transported partly by radiation and partly by conduction and convection: the glass radiates heat to the roof and walls, heat is conducted through the glass and walls to the atmosphere, and finally heat is lost from the outside of the feeder by radiation, conduction and convection. The dependence of the heat flow on the temperature difference ΔT can, of course, be expressed in a power series. This series, owing in particular to the presence of a radiation component, will also contain higher powers of ΔT. It follows, then, that the thermal resistance, i.e. the derivative of the heat flow with respect to ΔT, is not independent of ΔT and in an equivalent electrical circuit may only be represented by a pure resistance provided ΔT is practically constant. In our case this condition is satisfied, the temperature variations of the molten glass in the feeder being of the order of only 1 °C.

Not so much need be said about the other units of the loop. The thermometer, block *II*, can be treated as a capacitor (heat capacity) c which is charged by a current supplied by a voltage source via a resistance r. Here the input quantity is the voltage which represents the temperature of the glass tank (Table I, example 2). The transfer function for G_{II}, like that for G_{I}, therefore again has the form $(1 + j\omega\tau_{\mathrm{II}})^{-1}$, but the value of the time constant τ_{II} $(= rc)$ is very much smaller (e.g. half a minute).

The transfer function of block *IV*, the regulating valve, must define the relationship between the output signal from *III* and the flow of heat to the tank. There are two steps involved. The signal from *III* controls the valve in the gas pipe. The relationship between this signal and the corresponding change in the flow of gas will not, in general, be exactly linear. Secondly, the flow of gas to the burner determines the flow of heat to the glass; the relationship between these two quantities, which is partly governed by the size of the luminous cone in the flame [6]), will not always be linear either. For small variations, however, the behaviour of a non-linear element like block *IV* may permissibly be regarded as linear. Since a valve usually shows a certain lag, which may be characterized by one time constant, we have $G_{\mathrm{IV}} = (1 + j\omega\tau_{\mathrm{IV}})^{-1}$. Here again, τ_{IV} is small compared with τ_{I}.

Let us now briefly review the simplifications we have adopted. Firstly, of course, there were the approximations introduced to simplify the formulae for G_{I} and G_{IV}. Further, the block diagram as such (fig. 8) contains various approximations. In the first place we have disregarded the fact that, owing to the heat capacity of the burner, the heat flow to the glass does not respond instantaneously to a change in the gas supply. To take this into account we must add the factor $(1 + j\omega\tau_{\mathrm{V}})^{-1}$ to the transfer function of the whole loop. It is also a simplification to represent the glass by a single capacitance and to neglect the heat capacity of the wall. Finally, the temperature distribution of the glass is certainly not entirely uniform. There is no space to allow for all these factors here.

As a first approximation, however, our simplified treatment of the system's behaviour is justified. We may even go a step further and, since τ_{II} and $\tau_{\mathrm{IV}} \ll \tau_{\mathrm{I}}$, equate G_{II} and G_{IV} to unity. The block diagram then reduces to that of *fig. 9*, and the transfer function of the open loop is

$$KG = \frac{A}{1 + j\omega\tau_{\mathrm{I}}}, \quad \ldots\ldots \quad (14)$$

where $K = A$, and $G = (1 + j\omega\tau_{\mathrm{I}})^{-1}$.

As far as the *stability* of the system is concerned, however, the presence of the small time constants can *not* be neglected, for the variations of the controlled quantity are required to be very small, and therefore K must be given a very high value (see eq. (3)). The extent to which that is possible without endangering the stability of the system is in fact governed by the value of these small time constants [7]).

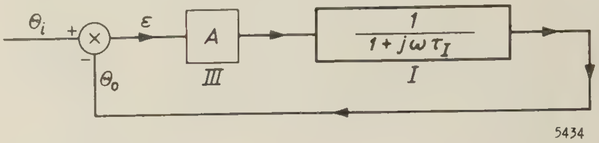

Fig. 9. Simplified form of block diagram of fig. 8, obtained by equating with unity the G function of all blocks for which $\tau \ll \tau_{\mathrm{I}}$. This approximation is permissible only if the gain factor A of *III* is not too high.

Control of the suspension temperature in the KEMA subcritical suspension reactor at Arnhem

Before finding the open-loop transfer function for the subcritical suspension reactor at Arnhem, we shall briefly recapitulate the operation of the control system, which has already been described in this journal [3]). A suspension of uranium oxide is pumped at a constant rate around the reactor circuit (see *fig. 10*). The pump P supplies 3-7 kW of energy to the fluid, and therefore some cooling is necessary even at the highest operating temperature. Stabilization of the temperature against variations in the power supplied by the pump and withdrawn by the cooler is effected by applying somewhat excessive cooling and by compensating the excess with the aid of a variable heater element V, which

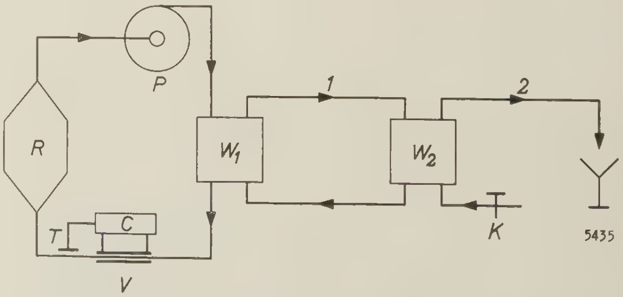

Fig. 10. Schematic representation of reactor circuit (left) and cooling circuits of the KEMA subcritical suspension reactor at Arnhem. R reactor vessel. P pump which circulates the suspension of uranium oxide around the reactor circuit in the direction of the arrows. T resistance thermometer. C control unit. V heater (regulating circuit). W_1 first heat exchanger. *1* primary cooling circuit. W_2 second heat exchanger. *2* secondary cooling circuit. K cooling-water valve.

---

[6]) See page 313 of reference [2]).

[7]) To be discussed in the forthcoming article mentioned in footnote [5]).

surrenders its heat directly to the suspension. The heater element is controlled by a thermometer T, which measures the temperature of the suspension. At equilibrium, the heater gives up about half its maximum power (5 kW), making it possible to offset variations of more than 2 kW in the power to be dissipated. The heater is simply a length of metal piping through which an electric current is passed. The temperature is measured with a Wheatstone-bridge resistance thermometer which delivers a voltage proportional to the difference between the measured and the desired temperature.

A block diagram of the control system is shown in *fig. 11*. The first block (A) again represents a linear amplifier. The transfer functions of blocks I and II together define the behaviour of the heater (i.e. the way in which the temperature Θ_t of the effluent suspension reacts to a variation in the power supplied to the heater), that of the last block (III) the behaviour of the thermometer itself. The disturbance Θ_s is a change in the temperature of the suspension, which is not detected until liquid of the wrong temperature reaches the thermometer. A fluctuation in the mains voltage must also be introduced at this point.

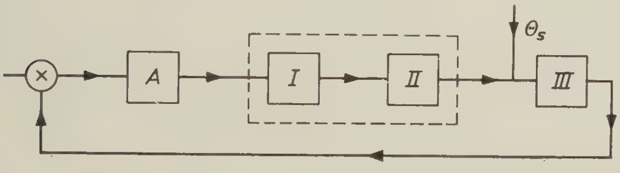

Fig. 11. Block diagram of temperature-control system in the Arnhem subcritical suspension reactor. Blocks I and II together represent the heater, block III the thermometer.

It may be asked whether fig. 11 does in fact represent the control loop, for there is another closed loop involved, viz. that of the circulating suspension. In order to show that the latter loop may be disregarded for our purposes, we recall that the control system has been designed to offset variations in the power delivered to the suspension by the pump and removed by the cooler [3]). The control equipment need only ensure that the fluid leaves the heater at the correct temperature. It is immaterial whether or not the fluid itself flows in an open or closed circuit.

Nor are our considerations affected by disregarding the influence of heat losses in other parts of the reactor circuit. Any such variation can be treated as a disturbance signal entering the loop at the same point as Θ_s, and can thus be regarded as a component of the latter.

To determine the transfer function of the heater it is convenient to divide the heating process into two stages, represented in fig. 11 by blocks I and II. The transfer function $K_I G_I$ defines the response of the temperature of the wall of the heater to a variation in the supplied power; the function $K_{II} G_{II}$ defines the response of the temperature of the effluent to a change in the temperature of the wall of the heater. In this connection we make two closely related simplifying assumptions. Firstly, we assume that the temperature of the heater pipe is uniform at all points, so that we may in fact refer to *the* temperature of the pipe. Secondly we assume that variations in the temperature of the effluent are negligible compared with the temperature variations shown by the pipe wall; in other words, we regard the heat capacity of the fluid as extremely high. In fact the suspension circulates fast enough for these assumptions to be correct. Otherwise, our division of the heater into two blocks would not be permissible, unless feedback were applied from block II to block I.

The transfer function $K_I G_I$ can most quickly be found from the equivalent electrical circuit shown in *fig. 12a*. The current I represents the power supplied, C_1 the heat capacity of the pipe, R_2 the thermal resistance at the boundary between pipe and suspension, C_2 the heat capacity of the suspension, V_1 the temperature of the pipe and V_2 the temperature of the fluid. Resistances R_1 and R_3 represent heat losses due to conduction and convection in the pipe and fluid mass in the rest of the reactor circuit. Measurements show that $C_1 \approx$ 500 J/°C, $C_2 \approx 400\ C_1$, $R_1 \approx 25 \times 10^{-3}$ °C/watt and $R_2 \approx 2.2 \times 10^{-3}$ °C/watt. We see that C_2 is in fact much larger than C_1. We can thus regard C_2 as short-circuiting R_3, in which case the diagram in

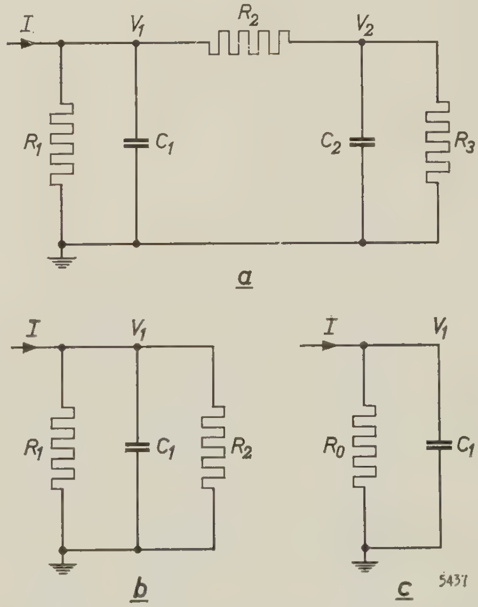

Fig. 12. *a*) Equivalent electrical circuit of heater operation. As $C_2 \gg C_1$, this can be simplified to *b*) or, by substituting R_0 for R_1 and R_2 in parallel, to *c*).

fig. 12*a* reduces to that in fig. 12*b*, and the latter may in turn be simplified to fig. 12*c* by replacing R_1 and R_2 by a single resistance R_0.

The transfer function of the first block is therefore equal to (see Table I, example 3):

$$\frac{V_1}{I} = R_0 \frac{1}{1 + \mathrm{j}\omega\tau_{\mathrm{I}}}, \quad . \quad . \quad . \quad . \quad (15)$$

i.e. $K_{\mathrm{I}} = R_0 = 2$ °C/kW and $G_{\mathrm{I}}(\mathrm{j}\omega) = (1 + \mathrm{j}\omega\tau_{\mathrm{I}})^{-1}$. The time constant τ_{I} is equal to R_0C_1 (one second).

The transfer function $K_{\mathrm{II}}G_{\mathrm{II}}$ (the change in the temperature of the fluid due to the change in the heater temperature) is found by determining the way in which the temperature of the effluent suspension fluctuates when the temperature of the pipe varies sinusoidally around the equilibrium value T_0 with an amplitude T_1 which is small compared to the average temperature difference between the pipe wall and the suspension. (Since the flow is highly turbulent, the temperature of the fluid is virtually identical in all points of a cross-section.)

If we consider a "disc" of suspension of thickness dx, moving at a constant velocity v through the pipe, we see that the disc must constantly encounter a different wall temperature in its passage through the pipe. The difference between this temperature and the equilibrium temperature of the wall is $T_1 \sin \omega(t_0 + x/v)$. Here t_0 is the time at which the disc entered the pipe, and x the distance which the disc has travelled in the pipe at the given moment. We shall now consider how much extra heat is supplied to the disc in its passage through the pipe as a result of this temperature difference. In the time dx/v during which the disc remains between x and x + dx it takes up an additional quantity of heat which gives rise to a temperature change proportional to

$$T_1 \sin \omega\left(t_0 + \frac{x}{v}\right) \times \frac{\mathrm{d}x}{v}. \quad . \quad . \quad . \quad (16)$$

The integral of this expression over the whole length l of the heater is proportional to the difference between the actual temperature which the disc has acquired by the time it reaches the end of the pipe and the temperature it would have acquired if the wall temperature had permanently been equal to T_0. This difference is thus proportional to

$$\int_0^l T_1 \sin \omega\left(t_0 + \frac{x}{v}\right) \frac{\mathrm{d}x}{v}, \quad . \quad . \quad . \quad (17)$$

which reduces to:

$$2\tau_{\mathrm{II}}\, T_1 \frac{\sin\omega\tau_{\mathrm{II}}}{\omega\tau_{\mathrm{II}}} \sin \omega\,(t_0 + \tau_{\mathrm{II}}), \qquad (18)$$

where $\tau_{\mathrm{II}} = l/2v$ (about 0.15 second). If we now consider the entire flow, i.e. a continuous series of discs for which the value of t_0 is successively larger by an amount dx/v, we may conclude that the variation of the temperature difference with time is given, apart from a constant factor, by expression (18) if t_0 is replaced by $(t - l/v)$, which is equal to $(t - 2\tau_{\mathrm{II}})$. Expression (18) then becomes:

$$2\tau_{\mathrm{II}}\, T_1 \frac{\sin\omega\tau_{\mathrm{II}}}{\omega\tau_{\mathrm{II}}} \sin \omega(t - \tau_{\mathrm{II}}) . \quad . \quad (19)$$

The corresponding complex quantity (we shall henceforth disregard the constant factor $2\tau_{\mathrm{II}}$) is:

$$T_1 \frac{\sin\omega\tau_{\mathrm{II}}}{\omega\tau_{\mathrm{II}}} \mathrm{e}^{\mathrm{j}\omega(t\quad\tau_{\mathrm{II}})}. \quad . \quad . \quad . \quad . \quad (20)$$

To find $G_{\mathrm{II}}(\mathrm{j}\omega)$ we divide (20) by the complex quantity corresponding to the input signal, $T_1\mathrm{e}^{\mathrm{j}\omega t}$, giving:

$$G_{\mathrm{II}}(\mathrm{j}\omega) = \frac{\sin\omega\tau_{\mathrm{II}}}{\omega\tau_{\mathrm{II}}} \mathrm{e}^{-\mathrm{j}\omega\tau_{\mathrm{II}}}. \quad . \quad . \quad . \quad (21)$$

It can be seen from eq. (21) that the time τ_{II} (which is known as the distance velocity lag) is of the nature of a transit time. This transit time causes a phase shift $\varphi = -\omega\tau_{\mathrm{II}}$ proportional to ω (*fig. 13*). Further, there is a frequency-dependent amplitude factor $(\sin \omega\tau_{\mathrm{II}})/\omega\tau_{\mathrm{II}}$ which is equal to unity at very low frequencies and is zero when $\omega\tau_{\mathrm{II}} = \pi$. In the latter case each disc traverses the heater in exactly one period, and thus takes up just as much energy in the one half as it gives up in the other half.

Block *III* in the diagram defines the behaviour of the resistance wire of the thermometer. This behaviour can be characterized to a good approximation by a single time constant τ_{III} (about 0.10 sec), so that

$$G_{\mathrm{III}}(\mathrm{j}\omega) = \frac{1}{1 + \mathrm{j}\omega\tau_{\mathrm{III}}}. \quad . \quad . \quad (22)$$

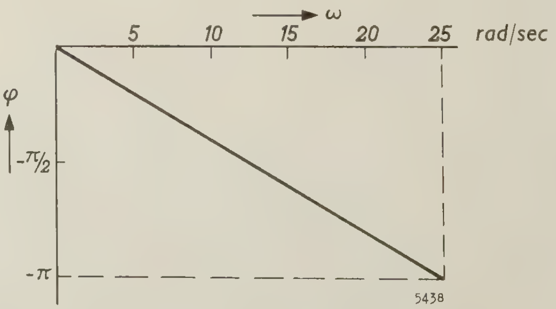

Fig. 13. Phase characteristic of the dissipation of heat by the heater in the circulating suspension (cf. eq. (21)). Because of the distance velocity lag τ_{II}, there is a phase shift proportional to ω. At the frequency $\omega = \pi/\tau_{\mathrm{II}}$ (≈ 25 rad/sec) the phase shift φ is $-\pi$.

The transfer function of the open control loop as a whole, which is equal to the product $AK_{\mathrm{I}}G_{\mathrm{I}}(\mathrm{j}\omega) \times K_{\mathrm{II}}G_{\mathrm{II}}(\mathrm{j}\omega)K_{\mathrm{III}}G_{\mathrm{III}}(\mathrm{j}\omega)$, is thus:

$$\frac{\Theta_{\mathrm{o}}}{\varepsilon} = AK^{\mathrm{I}}\, K_{\mathrm{II}}K_{\mathrm{III}}\, \frac{1}{1+\mathrm{j}\omega\tau_{\mathrm{I}}} \times \frac{\sin\ \omega\tau_{\mathrm{II}}}{\omega\tau_{\mathrm{II}}}\, \mathrm{e}^{-\mathrm{j}\omega\tau_{\mathrm{II}}} \times \frac{1}{1+\mathrm{j}\omega\tau_{\mathrm{III}}}. \quad . \ (23)$$

(Since the thermometer is not exactly at the end of the heater but somewhat further up in the pipe line, we should introduce into eq. (23) a second distance velocity lag, equal to the time τ_{IV} which the fluid needs to cover the relevant distance. However, since $\tau_{\mathrm{IV}} \ll \tau_{\mathrm{II}}$, this factor may be neglected.)

The frequency response curves derived from this transfer function are shown in *fig. 14*, and the Nyquist diagram in *fig. 15*. In *fig. 16* the factor P, the reciprocal of the deviation ratio, is plotted as a function of ω.

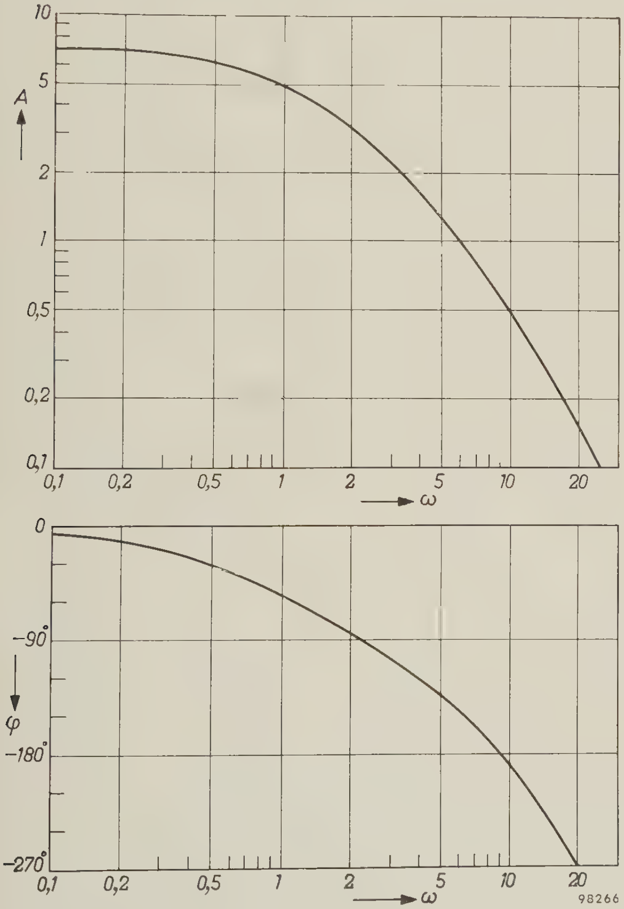

Fig. 14. Frequency response curves of the open control loop. *Top:* amplitude characteristic. *Bottom:* phase characteristic. At very low frequencies the gain is roughly 7. At the value of ω where the phase shift φ is 180°, the gain is less than unity.

A word should be added about the fact that the system is unable to correct high-frequency disturbances (see fig. 16). A sudden change in the valve controlling the cooling water in the secondary cooling circuit will not result in an immediate change in the temperature of the liquid flowing over the thermometer, nor will a sudden change in the mains voltage, i.e. in the power fed back to the heater (cf. fig. 12). Rapid variations of this kind thus give rise to relatively slow disturbances in the temperature of the suspension — which will, of course, be corrected — and are therefore unable to do any harm.

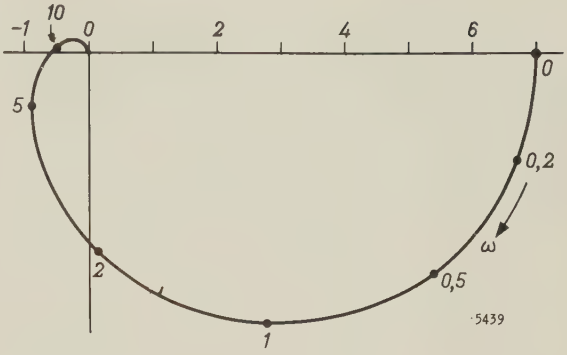

Fig. 15. Nyquist diagram pertaining to fig. 14.

In conclusion, some general remarks. The above examples have shown that it is very often not possible to calculate a loop transfer function exactly, and that approximations have to be made. In any case, exactly linear systems are never in fact encountered, so that our assumption of linearity is in itself an approximation. In cases where it is not possible to calculate the *KG* function at all, the frequency response curves can in principle be found from measurements. A sinusoidal disturbance is deliberately introduced, and the resultant variation of the output signal (Θ_{o} in fig. 1) is then recorded. This method cannot of course be used where the

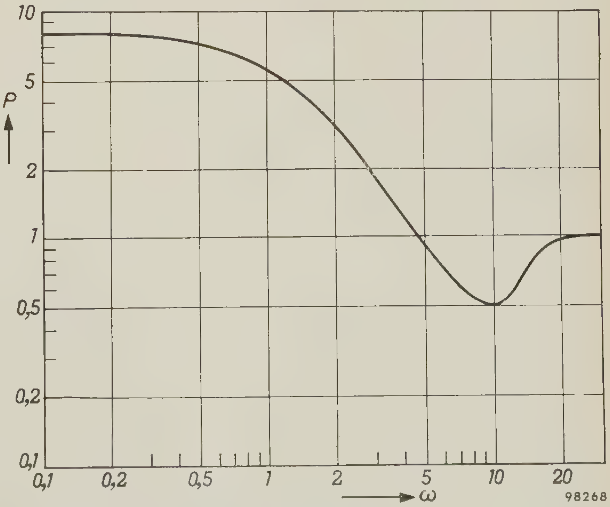

Fig. 16. The factor P (cf. fig. 4) as a function of ω, derived from fig. 15.

system is non-linear, or where the control loop cannot be opened. Considerable practical difficulties arise where long time constants are involved, because one then has to wait a very long time in each measurement before the switching transient has ended. In the latter case the object can sometimes be achieved by introducing a step-function disturbance and seeing how the system then behaves. From the step-function response thus obtained one can derive the frequency response curves, and from these find the values of the various time constants.

Summary. The theory of an automatic control system is formally similar to that of a negative-feedback amplifier. The behaviour of a feedback system, provided all its elements are linear, can be derived from the open-loop transfer function, $KG(\mathrm{j}\omega)$. This function is the quotient of the complex quantities corresponding to a sinusoidal input signal (angular frequency ω) and the resultant sinusoidal output signal. K is a constant factor. Disturbances are reduced by the factor $|1 + KG|$. The system is stable when the curve representing KG in the complex plane does not enclose the point $(-1,0)$. The KG functions are calculated for 1) a tank with water flowing in and out, 2) the temperature control system for a glass-furnace feeder, and 3) the temperature control system for the subcritical suspension reactor at Arnhem. The elements of a control loop frequently have a transfer function of the form $KG(\mathrm{j}\omega) = K(1 + \mathrm{j}\omega\tau)^{-1}$.

A SIMPLE ANALOGUE COMPUTER FOR DETERMINING THE COLOUR POINT OF A LIGHT SOURCE

by B. van der WAAL *).

535.651.1

Determining the "colour point" of a light source calls for a series of simple but laborious computations. The computer described below performs this work rapidly and automatically; the CIE-distribution coefficients, which define the spectral sensitivity of the eye of a "standard observer", are built into the machine.

One of the principal characteristics of a light source is the colour of the light it emits. The colour can be objectively specified [1]) with the aid of three quantities X, Y and Z, defined as

$$\left.\begin{aligned} X &= \int S(\lambda)\,\bar{x}(\lambda)\,\mathrm{d}\lambda, \\ Y &= \int S(\lambda)\,\bar{y}(\lambda)\,\mathrm{d}\lambda, \\ Z &= \int S(\lambda)\,\bar{z}(\lambda)\,\mathrm{d}\lambda. \end{aligned}\right\} \quad \ldots \ldots \quad (1)$$

In these equations $S(\lambda)$ is the relative spectral energy distribution of the radiated light; $\bar{x}(\lambda)$, $\bar{y}(\lambda)$ and $\bar{z}(\lambda)$ are the CIE-distribution coefficients, which define the spectral sensitivity of the eye as laid down in 1931 for the "colorimetric standard observer" by the International Commission on Illumination (CIE). The coefficients are so chosen that the values of $\bar{y}(\lambda)$ are identical with those of the relative luminous efficiency $V(\lambda)$. The maximum values of these coefficients occur at wavelengths in the red, green and blue parts of the spectrum, respectively (see *fig. 1*).

It is however usually more convenient to specify the colour of a light source by the ratios of X, Y and Z to their sum:

$$\left.\begin{aligned} x &= \frac{X}{X+Y+Z}, \\ y &= \frac{Y}{X+Y+Z}, \\ z &= \frac{Z}{X+Y+Z}. \end{aligned}\right\} \quad \ldots \ldots \quad (2)$$

As the sum $x + y + z$ is 1, two of these values are of course sufficient to specify a colour. Any colour can thus be represented by a point in an x-y diagram, as in the CIE *chromaticity diagram* or colour triangle (*fig. 2*). The colour points of monochromatic light lie on a horseshoe-shaped curve called the *spectrum locus*. The straight line joining the ends of the spectrum locus, the "purple line", represents the pure (saturated) purples, mixtures of red and violet radiations. In the centre lies the "white point" E, where x, y and z are equal. The other points may be regarded as colour points of a mixture of white light with a spectral colour or with a colour on the purple line.

---

*) Lighting Division, Eindhoven.

[1]) See W. de Groot and A. A. Kruithof, The colour triangle, Philips tech. Rev. **12**, 137-144, 1950/51; F. W. de Vrijer, Fundamentals of colour television, Philips tech. Rev. **19**, 86-97, 1957/58; P. J. Bouma, Physical aspects of colour, Philips Technical Library, 1947.
The notation used in these articles differs somewhat from current usage, which conforms more or less with the official recommendations of the International Commission on Illumination; see "International Lighting Vocabulary", publication CIE 1-1-1957.

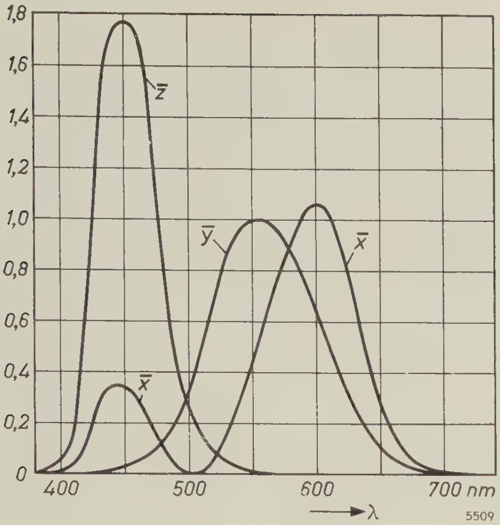

Fig. 1. The CIE-distribution coefficients $\bar{x}(\lambda)$, $\bar{y}(\lambda)$ and $\bar{z}(\lambda)$, giving the equal-energy distribution curves in the CIE system.

(A chromaticity chart showing the actual colours corresponding to various points can be found in the first article referred to in note [1]).

The determination of the colour point of a light source

The method of finding the colour point of a given light source follows directly from equations (1) and (2). The value of $S(\lambda)$ for the light is measured with a spectrophotometer at a series of wavelengths rising in steps of 10 nm from 385 to 735 nm. (1 nm = 10^{-9} m.) To find X the values thus measured are multiplied by the values of $x(\lambda)$ corresponding to the same wavelengths and the products are then added. (One should really multiply by the width of the wavelength interval used in the measurement, but as we are only concerned with the ratios of X, Y and Z, we have omitted to do so here.) The values of Y and Z are calculated in the same way, after which x and y are determined by two division operations from equation (2). The computation of a single colour point thus involves about 100 multiplications, followed by three additions and two divisions.

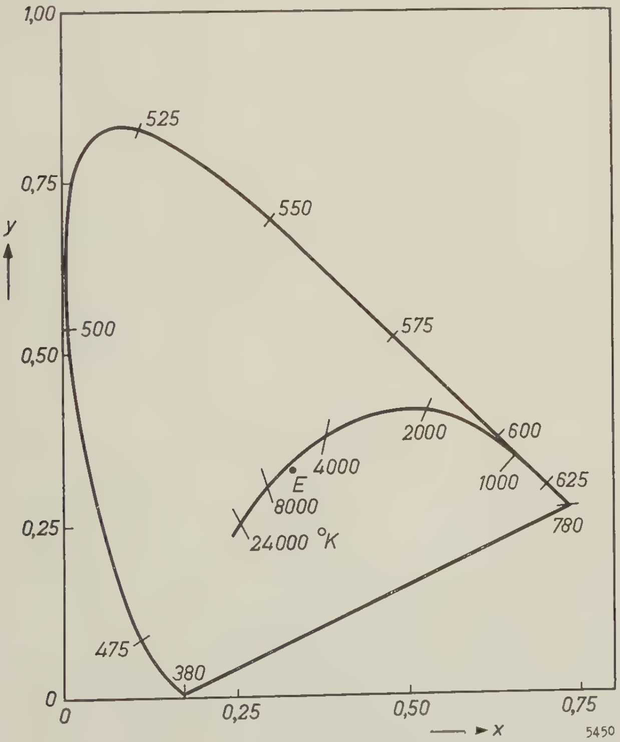

Fig. 2. The CIE chromaticity diagram in x-y coordinates. On the spectrum locus (curve of the spectral colours) the corresponding wavelengths are given in nm. (1 nm = 10^{-9} m.) E is the "white point". The curve inside the spectrum locus joins the colour points of a black-body radiator at different temperatures.

A simple analogue computer has been designed for performing these operations automatically. The principle is illustrated in *fig. 3*. For every wavelength λ_n at which $S(\lambda)$ is measured there is a circuit consisting of three resistors R_{xn}, R_{yn} and R_{zn}, whose respective values are inversely proportional to $\bar{x}(\lambda)$, $\bar{y}(\lambda)$ and $\bar{z}(\lambda)$ at that wavelength. A voltage derived from an accumulator B_1 via a potentiometer R_{pn} is applied to each resistor, the value of the voltage being proportional to the measured value of $S(\lambda)$ (for this purpose the meter M, used as a voltmeter, can be connected to each potentiometer in turn). The currents through the resistors are then proportional to $S(\lambda_n)\bar{x}(\lambda_n)$, $S(\lambda_n)\bar{y}(\lambda_n)$ and $S(\lambda_n)\bar{z}(\lambda_n)$, respectively. The sum of the currents through all resistors R_{xn} is

$$\Sigma S(\lambda_n)^{-}(\lambda_n)$$

and is therefore proportional to X. The sums of the currents through R_{yn} and R_{zn} are similarly proportional to Y and Z respectively, the constant of proportionality being the same in all cases.

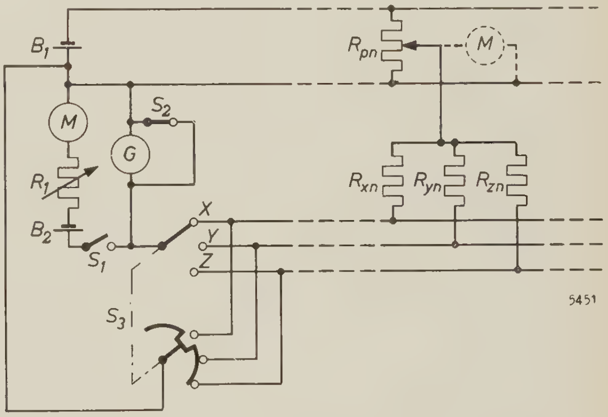

Fig. 3. Principle of the computer circuit for determining the colour point of a light source.

In measurements on tubular fluorescent lamps the energy at the wavelengths of the five mercury lines is determined in addition to $S(\lambda)$ at the wavelengths mentioned. The computer contains similar circuits for these wavelengths too, giving a total of 41.

When all 41 potentiometers have been set to the appropriate values, the three currents are determined by a null method, using a circuit consisting of a galvanometer G, a battery B_2, the meter M (now used as an ammeter) and a variable resistance R_1. The switch S_1 is closed, S_2 opened, and S_3 turned first to position X. The current through G is now made zero by adjusting R_1; X can then be read off from meter M. The values of Y and Z are found in the same way, with S_3 in positions Y and Z respectively.

Switch S_3 was given the form shown in fig. 3 to ensure that all resistors pass current both during the adjustment of the voltages and the measurement of the currents. If current were to flow through only one of the three sets of resistors (in which case only the top half of S_3 would be needed) the currents through the potentiometers would change when S_3 was switched over, and the voltages would have to be reset. With this arrangement, however, one setting serves for all three measurements. A photograph of the computer can be seen in *fig. 4*.

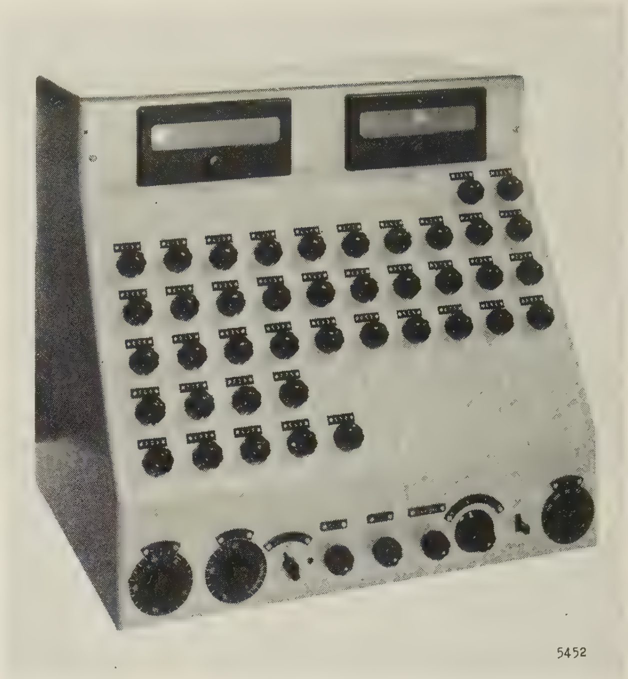

Fig. 4. Photograph of the colour-point computer. The sloping panel contains the potentiometer controls for presetting the measured energy values. Above left, the meter M shown in fig. 3, and right, the galvanometer G. The bottom row contains, among other things, the controls of the variable resistors used in the determination of X, Y and Z.

Other uses for the computer

The computer can be used for many other calculations that involve multiplication operations with the CIE-distribution coefficients or simply with the relative luminous efficiencies $V(\lambda)$. For example, to find the distribution of luminous flux over various wavelength regions, the measured values of the relative spectral energy distribution $S(\lambda)$ are multiplied by the values of $V(\lambda)$ for the wavelengths concerned, and the products for the various wavelengths are added.

The computer is also useful for "normalizing" the relative spectral energy distribution $S(\lambda)$. This is done when it is necessary for irradiation purposes (e.g. the irradiation of plants) to know the *absolute* value of the radiant power delivered to a surface by a light source in a particular range of wavelengths. A spectral energy distribution is then needed which gives the absolute instead of the relative values for the surface in question.

These values might be determined by the following procedure. The total radiant power P incident on the surface is measured and divided by $\int S(\lambda)\mathrm{d}\lambda$, an integral proportional to the total radiant power received by the photometer in the measurement of $S(\lambda)$. Multiplying the values of $S(\lambda)$ by this factor $P/\int S(\lambda)\mathrm{d}\lambda$ gives the absolute distribution required:

$$\frac{S(\lambda)}{\int S(\lambda)\mathrm{d}\lambda}\,P. \quad \ldots\ldots \quad (3)$$

$S(\lambda)/\int S(\lambda)\mathrm{d}\lambda$ is called the *normalized distribution.* To find from this the absolute distribution on an arbitrary surface the values are multiplied by the measured total radiant power through that surface.

The actual procedure is somewhat different. For practical reasons it is easier to measure the *luminous flux* on a surface than the radiant power. The normalized energy distribution is then found by dividing $S(\lambda)$ by

$$K \int S(\lambda)V(\lambda)\mathrm{d}\lambda\,. \quad \ldots\ldots \quad (4)$$

(This integral is proportional to the total luminous flux received by the photometer in measuring $S(\lambda)$; K is the luminous efficiency of radiation, which is about 680 lumen/W.) The normalized energy distribution found in this way is expressed in μW/lumen per 10 nm. The absolute distribution is found from it by multiplying by the measured luminous flux on the surface.

Since $V(\lambda)$ and $\bar{y}(\lambda)$ are identical, the integral in eq. (4) is equal to the integral Y in eq. (1), and can thus be determined with the computer in the same manner as the colour point. Now, however, the absolute value of Y must be known, and therefore the computer is calibrated by determining Y with it for an energy distribution in which this quantity is known. For this purpose we used the equi-energy spectrum, for which Y can be easily computed.

Summary. After a brief explanation of the CIE chromaticity chart, a simple analogue computer is described with which the colour point of a light source can be determined from the relative spectral energy distribution $S(\lambda)$, measured at a series of wavelengths rising in steps of 10 nm. These values are multiplied by the corresponding CIE-distribution coefficients $\bar{x}(\lambda)$, $\bar{y}(\lambda)$ and $\bar{z}(\lambda)$. The products $S(\lambda)\bar{x}(\lambda)$, $S(\lambda)\bar{y}(\lambda)$ and $S(\lambda)\bar{z}(\lambda)$ are all added to find the values of X, Y and Z which define the chromaticity of the light. For every wavelength at which $S(\lambda)$ is measured, the computer contains three resistors whose values are proportional to $1/\bar{x}(\lambda)$, $1/\bar{y}(\lambda)$ and $1/\bar{z}(\lambda)$. A voltage proportional to the measured value of $S(\lambda)$ is applied to these resistors. The currents then flowing through them are proportional to the products mentioned, and are added in the computer. Other operations which can be carried out with the aid of the computer include the normalizing of a relative spectral energy distribution.

ANALYSIS OF RESIDUAL GASES IN TELEVISION PICTURE TUBES WITH THE AID OF THE OMEGATRON

by J. van der WAAL *) and J. C. FRANCKEN *).

621.385.832.032.94:621.384.83

The omegatron, in a new design recently described in this journal, is a particularly useful mass spectrometer for the quantitative analysis of residual gases. Analyses of this kind have provided valuable information on processes inside a television picture tube during manufacture and in operation.

In a properly functioning television picture tube the total residual gas pressure should be less than 10^{-5} torr (1 torr = 1 mm Hg). The composition of the residual gas is also an important consideration, for one kind of gas can be more harmful than another.

The life of the cathode in a picture tube is particularly dependent on the types of gas present. The composition of the residual gas in an evacuated and sealed-off tube changes continuously, owing to the desorption and adsorption of gases by the various components. The composition of this residual gas can be determined with a mass spectrometer.

It is important that the spectrometer used should have a small volume and that it should release little gas compared with the picture tube. A mass spectrometer found especially suitable for this purpose is the omegatron.

The omegatron had already been used in 1953 for *qualitative* analysis of residual gases in sealed-off cathode-ray tubes [1]). As recently mentioned in this journal, an omegatron has now been designed which is also suitable for quantitative analyses [2]). Its use for analysing the residual gases in television picture tubes will be described in this article. The operation of the omegatron was discussed at length in the above-mentioned article. For convenience, we shall briefly recapitulate this discussion here.

Principle of the omegatron

A perspective sketch of the omegatron in its simplest form is shown in *fig. 1*. The narrow beam of electrons from the cathode K is parallel to a uniform magnetic field. The collision of electrons with gas molecules gives rise to ions. If the latter have a velocity component perpendicular to the direction of the magnetic field, they describe circular paths perpendicular to the static magnetic field. The radii of these paths are given by the equation:

$$r = \frac{m}{e}\,\frac{v_0}{B}, \qquad \dots\dots \quad (1)$$

where m is the mass of the ion, e its charge, v_0 the component of the velocity perpendicular to the direction of the magnetic field, and B the magnetic induction. The angular frequency ω_c of the revolution of the ion is

$$\omega_c = \frac{e}{m}B, \qquad \dots\dots\dots \quad (2)$$

and the period of revolution is therefore independent of the velocity v_0. An RF field $\hat{E}_{hf} \sin \omega_0 t$ is applied at right angles to the magnetic field. If the angular frequency ω_0 of that field is made equal to the angular frequency ω_c of a given kind of ion, the result

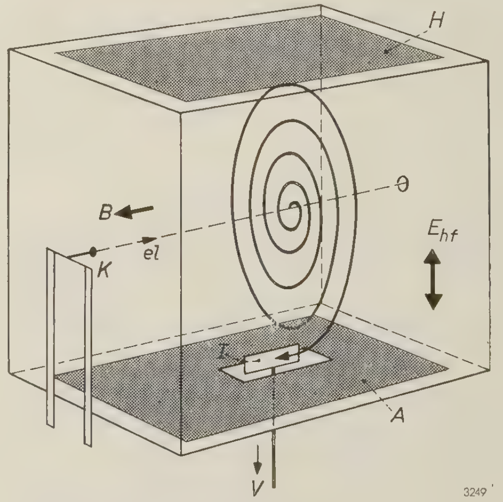

Fig. 1. Perspective sketch of a simplified omegatron. B indicates the direction of the magnetic induction, E_{hf} the direction of the RF field. The figure illustrates the spiral path described by an ion. K cathode, which emits the ionizing beam of electrons *el*. A and H are the electrodes to which the RF voltage is applied. I ion collector. V connection to amplifier.

---

*) Electron Tubes Division, Eindhoven.

[1]) J. Peper, Philips tech. Rev. **19**, 218-220, 1957/58.

[2]) A. Klopfer and W. Schmidt, Philips tech. Rev. **22**, 195-206, 1960/61 (No. 6).

is a condition of resonance. The resonating ions then describe spiral paths of uniformly increasing radius. They are caught on a suitably placed collector electrode, and the ion current, i.e. the number of ions collected per unit time, is detected with the aid of a sensitive amplifier.

Ions having a different mass but the same charge as the resonating ions, i.e. ions with a different value of e/m, are periodically accelerated and decelerated by the RF field. The radius of the orbits described by these ions alternately increases and decreases, but the maximum value generally remains smaller than the distance between the point of origin of the ions and the collector. Such ions do not therefore contribute to the measured current. To discriminate in this way between two kinds of ions, their mass difference Δm must exceed a specific minimum value. The ratio $m/\Delta m$ is called the resolution of the omegatron.

The pressure of each component of the gas mixture can be found by varying the frequency ω_0 of the RF field and measuring the ion current for the various mass numbers. If the relationship between ion current and pressure is reproducible, the partial gas pressure for any mass number can be determined from the ion current. This relationship will be reproducible when all resonating ions reach the collector electrode. That is only the case when the total gas pressure in the omegatron is less than 10^{-5} torr; otherwise ions are lost by collision with gas molecules. Further, ions in resonance should not strike other electrodes. This can be prevented by fitting side plates and appropriately choosing the potential distribution inside the omegatron, as described in the article quoted [2]). A photograph of the omegatron used for this investigation is shown in *fig. 2*.

Experimental set-up

In all the experiments described here, use was made of a permanent magnet having a magnetic induction of 0.44 Wb/m². The RF voltage was 1 volt r.m.s. This voltage was taken from a Philips signal generator, type GM 2653. The electron current of the omegatron was stabilized. After amplification, the ion current was measured with a highly stable DC amplifier with negative feedback [3]). The smallest measurable current was 10^{-14} A.

The resolution $m/\Delta m$ of the omegatron depends markedly on the magnitude of the magnetic induction B, as appears from the equation:

$$\frac{m}{\Delta m} = \frac{e\,B^2 S_0}{2\,\hat{E}_{\mathrm{hf}}\,m}, \qquad (3)$$

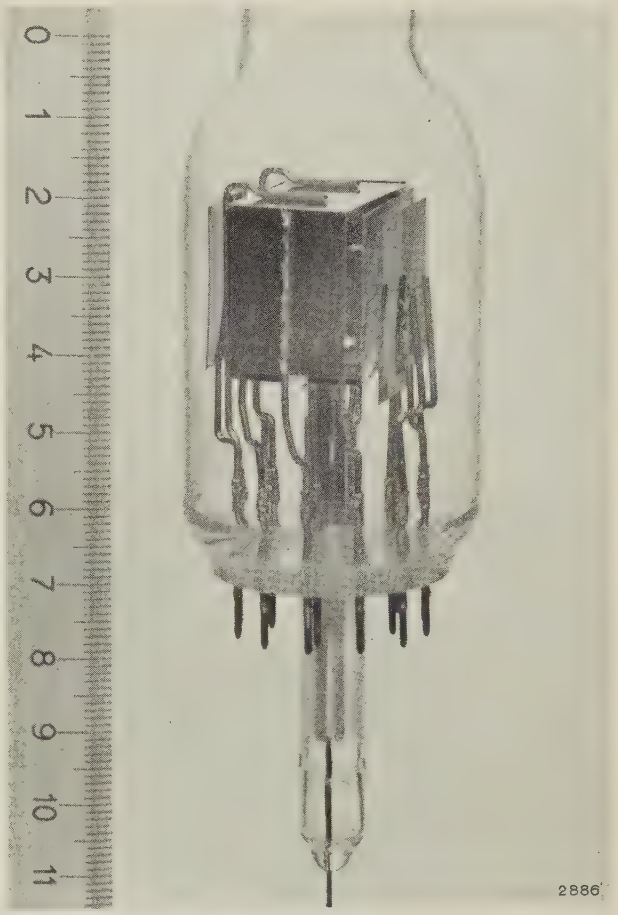

Fig. 2. The omegatron with side plates in a glass envelope. The cathode is on the right, and on the extreme left is the collector for the electrons which have traversed the omegatron. The ions formed in the space inside the omegatron move to the ion collector. This is connected to the central metal pin fused into the glass tube and projecting below it.

where S_0 is the distance from the point where the ion originated to the ion collector and $\hat{E}_{\mathrm{hf}}$ is the amplitude of the RF field.

The resolution of the omegatron can easily be derived from the equation given in the literature for the radius r of the ion orbits [4]):

$$r = \frac{\hat{E}_{\mathrm{hf}}}{B\varepsilon} \sin \frac{\varepsilon}{2} t, \qquad (4)$$

where ε is the difference between the resonance frequency ω_c of an ion having mass m and charge e and the frequency ω_0 of the applied RF field: $\varepsilon = |\omega_0 - \omega_c|$. It is assumed that $\varepsilon \ll \omega_c$. The ions cannot pass beyond a circle of radius

$$r_{\max} = \hat{E}_{\mathrm{hf}}/B\varepsilon\,. \qquad (5)$$

If $\varepsilon \leqslant \hat{E}_{\mathrm{hf}}/BS_0$, then $r_{\max} \geqslant S_0$ and ions of resonance frequency ω_0 reach the ion collector even though the frequency ω_0 of the RF field differs from ω_c. If $\varepsilon > \hat{E}_{\mathrm{hf}}/BS_0$, $r_{\max} < S_0$ and these ions do not arrive on the collector. It follows, then, that ions having a resonance frequency ω_c will continue to fall on the collector while the frequency of the RF field is varied between $\omega_0+\varepsilon$ and $\omega_0-\varepsilon$. It will then only just be possible to discriminate completely between a mass m and a mass $m+\Delta m$, provided the difference $\Delta\omega_c$ between the resonance frequencies of the two masses is equal to 2ε. We can thus write the resolution as

---

[3]) J. Pelchowitch, Philips Res. Repts **9**, 1, 1954.

[4]) H. Sommer, H. A. Thomas and J. A. Hipple, Phys. Rev. **82**, 697, 1951.

$$\frac{m}{\Delta m}=\frac{\omega_c}{\Delta\omega_c}=\frac{\omega_c}{2\varepsilon}=\frac{eB^2S_0}{2\,\hat{E}_{\mathrm{hf}}\,m}\,. \quad . \; . \; . \; . \quad (6)$$

In the experimental arrangement used the resolution is theoretically (i.e. according to equation (6)) such that two kinds of ions whose mass difference is $\Delta m = 1$ can be completely separated if the mass number m is not greater than 34. In actual fact this was found to be the case up to $m = 23$. In order to improve the resolution, we have recently obtained a permanent magnet whose magnetic induction B is 0.92 Wb/m². *Fig. 3* shows a photograph of this magnet together with the other equipment used. The picture tube under investigation is held in an adjustable yoke. The distance between the poles of the magnet is 5.0 cm, and the diameter of the pole pieces is 13.0 cm. At a distance of 2.0 cm from the centre the variation in the magnetic induction is only 0.1%. Theoretically the resolution is now such that two kinds of ions with $\Delta m = 1$ can be completely separated if m is not greater than 73. Experimentally, effective separation is found up to $m = 49$, which means that for example propane gas (C_3H_8, mass number 44) can be fully distinguished from its "neighbours" using the large

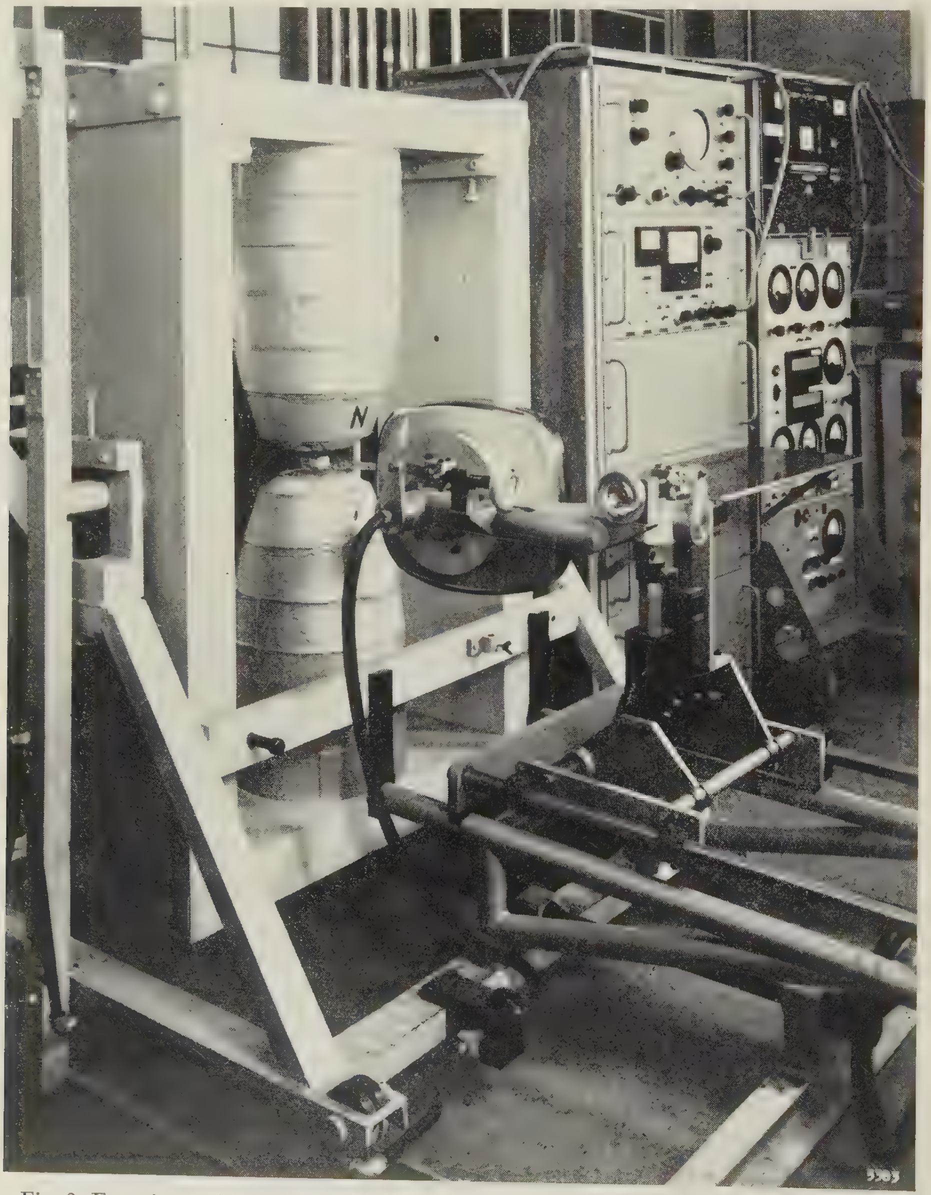

Fig. 3. Experimental set-up, consisting of a permanent magnet (magnetic induction B = 0.92 Wb/m²), a DC amplifier for the ion current, a Philips signal generator, type GM 2653, which supplies the RF voltage, and ancillary equipment for the other voltages needed for the omegatron. The television picture tube under investigation is connected to an omegatron located between the pole pieces of the magnet.

magnet; but not when using the small magnet. *Fig. 4* shows the spectrum of a mixture of propane and a trace of methane. This spectrum was recorded using the magnet with induction $B = 0.44$ Wb/m^2.

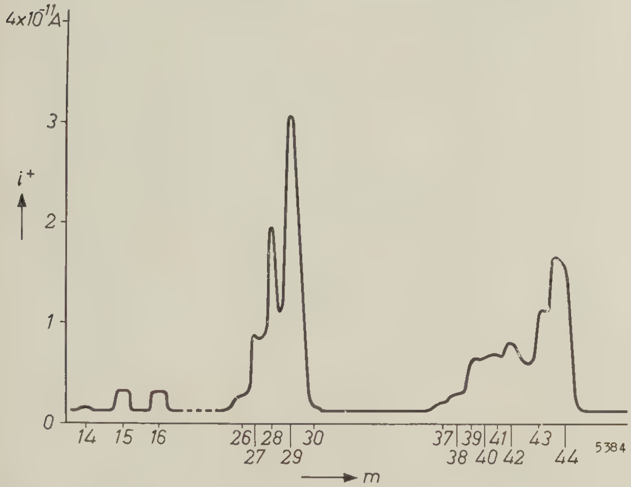

Fig. 4. Mass spectrogram of residual gases in a television picture tube, showing ion current i^+ of omegatron as a function of the preset mass number m. The tube contains propane C_3H_8 and a small quantity of methane CH_4. The RF voltage was 1 V. The magnet used for this recording has a magnetic induction $B = 0.44$ Wb/m^2.

Fig. 5 shows the same spectrum, but now with an induction $B = 0.92$ Wb/m^2. The improved resolution is particularly noticeable for the mass numbers 43 and 44.

Gas analyses on picture tubes in various stages of manufacture

In the manufacture of television picture tubes it is important to know not only the composition of the residual gases in the finished tube, but also which parts of the tube contribute most to this residue, and what gases they contribute. This information is obtained by studying unfinished tubes, i.e. tubes which have not yet been fitted with a fluorescent screen and/or other components. Analyses are also carried out after the various operations following seal-off.

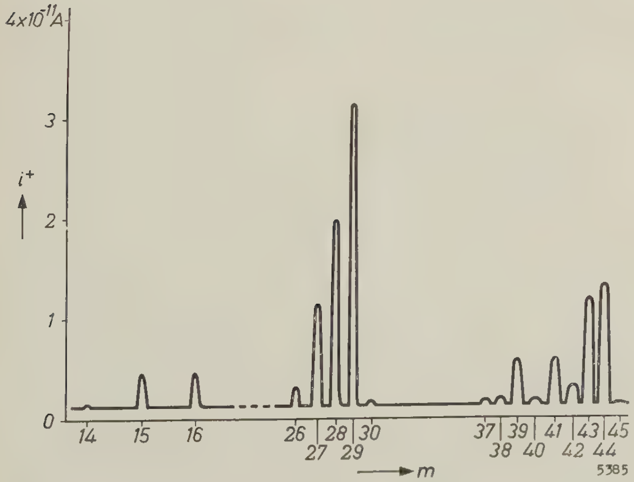

Fig. 5. The same mass spectrum as in fig. 4, but now using a magnet with $B = 0.92$ Wb/m^2. The voltages applied to the omegatron were the same as in the previous analysis. The resolution is substantially improved.

In all cases an omegatron is fixed to the side of the tube immediately below the screen. First of all we investigate the glass bulb of a picture tube which contains only an unevaporated barium getter, but otherwise none of the "normal" components, such as fluorescent screen and electron gun. In addition to the omegatron a Philips ionization gauge, type 53 EM [5]), is sealed to the tube. The only operation undergone by the tube is evacuation for two hours on an oil-diffusion pump. During this process the tube is heated for 20 minutes at 400 °C and allowed to cool to about 100 °C, after which it is sealed off. It is assumed that a more or less stationary state sets in 20 hours after seal-off. The gas composition is then measured with the omegatron. The gases found are hydrogen, methane, water vapour, carbon monoxide and carbon dioxide. Next, the getter is evaporated and a further measurement is made. The chemically active gases have now been absorbed by the getter, and in their place the tube contains a great deal of hydrocarbons, probably due to reactions between water vapour and carbon in the getter. The hydrocarbons are not taken up by the getter. A certain amount of argon, absorbed by the barium getter during its manufacture, is also found. The ionization gauge is now switched on for 15 minutes. The pumping action of this gauge depends on two effects. In the first place, hydrocarbons are decomposed at the hot cathode, which is at a temperature between 1500° and 2000°C. The fragments react with the getter, thereby reducing the pressure. Secondly, the electron current of 2.5 mA produces ions in the gas, which are captured by the collector and thus removed from the gas. This too results in a pressure drop. At the end of the 15 minutes the ion gauge is switched off and the tube is left for 14 days without anything being done to it. At the end of this period only a very slight increase in pressure is found.

In *fig. 6* the results of gas analyses done at four different times are compared: *a*) before and *b*) after evaporation of the getter, *c*) after 15 minutes of drawing current in the ionization gauge, and *d*) after 14 days. In the right-hand column the getter had been preheated (subjected to previous degassing) in the left-hand column it had not. The initial pres-

---

[5]) E. Bouwmeester and N. Warmoltz, Philips tech. Rev. 17, 121-125, 1955/56.

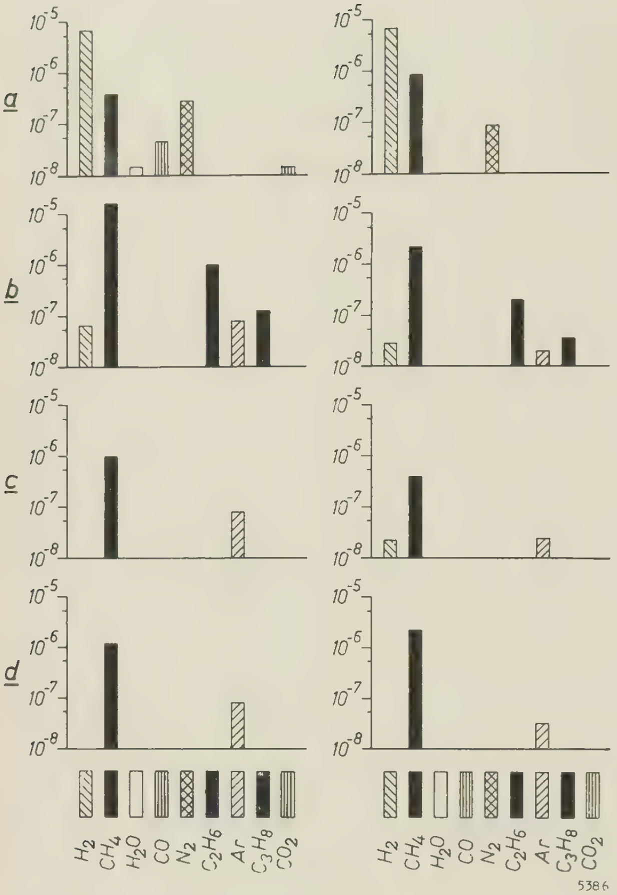

Fig. 6. Composition of the residual gases in unworked bulbs of television tubes. *a*) Before evaporation of barium getter; *b*) after evaporation of getter; *c*) after Philips 53 EM ionization gauge had drawn a current of 2.5 mA for 15 minutes; *d*) 14 days later. In the left column the getter had not been preheated; in the right column it had. Scale for partial pressures in torrs (mm Hg), likewise in following figures.

sure is lower when the getter has been preheated, but after 14 days no difference is to be found.

Fig. 7 shows a comparison between four different bulbs analysed at four different phases in the production process, without the getter having been evaporated. The first bulb (*a*), as in the previous case, contains no screen or components. The second (*b*) has been provided with a fluorescent screen, and in the third (*c*) the screen has been given the conductive coating of aluminium. The last bulb (*d*) also contains the electron gun. The cathode in the gun was degassed and activated when the bulb was still on the oil-diffusion pump. All four bulbs were subjected to the pumping process described above. Twenty hours after seal-off the gas composition was determined with the omegatron. It is noticeable that the hydrogen pressure is lower and the nitrogen and argon pressures higher in the second bulb. The hydrogen has probably been taken up by the screen, and the higher nitrogen and argon pressure is presumably due to the uptake of these gases from the atmosphere during the production of the screen. Bulb *c* differs hardly at all from bulb *b*, but the finished tube with the electron gun has a lower nitrogen pressure and a higher carbon monoxide pressure. The carbon dioxide pressure has also gone up, probably as a result of the gas given off by the oxide cathode.

After evaporation of the getter in the finished tube the gas composition changes radically, and in most tubes the residual gases consist solely of methane and argon. In some tubes, however, other hydrocarbons are found, but with a much lower partial pressure than methane.

Fig. 8 shows how the composition of the residual gases in a finished picture tube changes during operation. Measurements were started twenty hours

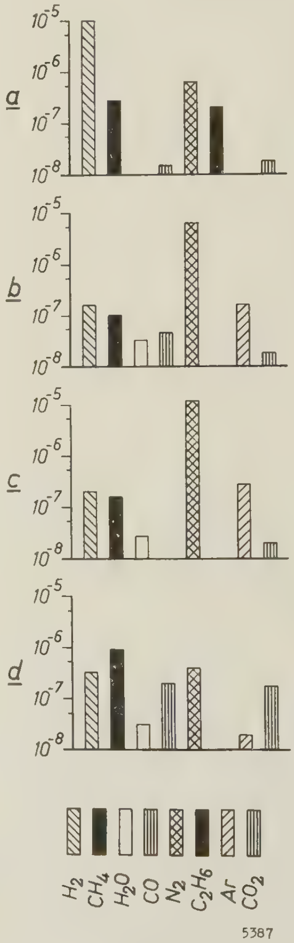

Fig. 7

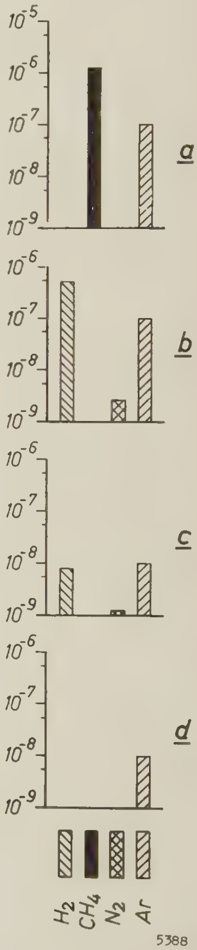

Fig. 8

Fig. 7. Composition of residual gases in picture tubes in various stages of production. *a*) Unworked glass bulb; *b*) bulb with fluorescent screen; *c*) bulb with fluorescent screen and conductive aluminium coating; *d*) tube complete with electron gun. The getter was not evaporated in any of the tubes.

Fig. 8. Composition of residual gases in a finished picture tube at four different times. *a*) 20 hours after seal-off, with the cathode cold; very little change occurs when the cathode is raised to working temperature. *b*) during the first hour of screen bombardment; *c*) after 250 hours of screen bombardment, measured during operation; *d*) immediately after switching the tube off.

after seal-off (*a*). While the cathode is heating up, very little change is found, but as soon as the screen is scanned by an electron beam, the nitrogen and hydrogen pressures increase and the hydrocarbons vanish (*b*). After scanning of the screen for 250 hours with an electron current of 275 μA — the electron energy being 16 keV — the hydrogen and nitrogen pressures are found to have decreased (*c*). After scanning is stopped, the only residual gas which can be detected is argon (*d*). The pumping speed of the getter film is apparently not high enough to deal initially with the large production of hydrogen and nitrogen. We shall return later to the very sharp drop in the quantity of hydrocarbons at the beginning of the scanning of the screen.

Breaking open the picture tubes under vacuum

We have seen how the composition of the residual gases in picture tubes can be determined by connecting an omegatron to the tube at the outset. It may happen, however, that a tube from normal production is not working properly because the gas pressure is too high. In such a case we want to be able to attach the omegatron to the rejected tube to ascertain the gas responsible for the fault.

This is done in the following way. First of all an area 5 mm in diameter in the neck of the bulb near the electron gun is ground down with an ultrasonic drill to a thickness of only 0.5 mm [6]). A thin glass tube is cemented round the weakened area with epoxy resin. The glass tube is connected to a pump system incorporating an omegatron, and a metal weight is introduced into the tube. The resin is hardened by heating at about 100 °C for half an hour, resulting in a strong vacuum-tight joint. At a suitable moment the weight, which has a sharp steel point and can be moved with a magnet, is made to break the thin glass wall, thus establishing communication between picture tube and omegatron. *Fig. 9* shows a diagram of the whole arrangement. The part shown enclosed in the dotted lines is degassed for 15 hours at 400 °C before being connected to the rest of the system. At the same time the glass connecting tube is heated by hot wires to 200 °C. During this process the epoxy resin does not get hotter than 100 °C, and the picture tube as a whole remains at room temperature. After 15 hours on the diffusion pump and outgassing, the pressure is reduced to a value between 1×10^{-8} and 5×10^{-8} torr. The residual gases are then hydrogen, nitrogen, carbon dioxide and sometimes a small amount of water vapour.

After the system has been cooled to room temperature, the high-vacuum valve K_1 is closed. This is a glass valve containing no grease and is closed by means of a magnet. Once the glass membrane between the system and the picture tube has been broken, the gas content of the tube can be analysed with the omegatron.

For this method to have any value the gas desorption of the epoxy resin must obviously be low. In the system without epoxy resin obtained by sealing off the glass tube above the connection to the picture tube, a pressure of 10^{-9} torr can

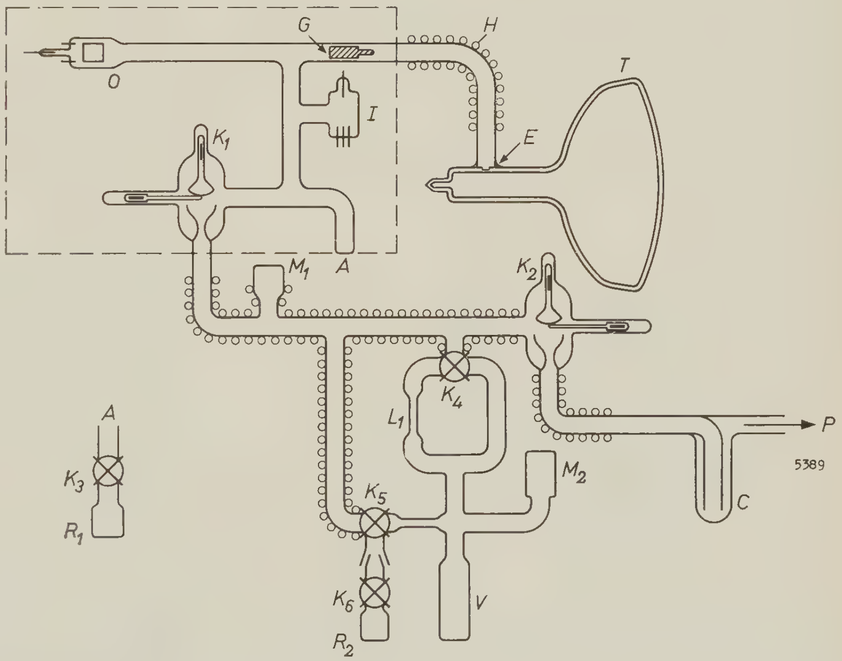

Fig. 9. System for breaking open a television tube and analysing the residual gases. A glass tube is cemented with epoxy resin *E* round a spot in the neck of a picture tube *T* where the wall has been ground very thin. The connecting tube is degassed by a heater coil *H*. The part of the system inside the broken line can be outgassed in an oven at 400 °C. This part comprises an omegatron *O*, an ionization gauge *I*, a weight *G* and a glass high-vacuum valve K_1. M_1 Penning gauge. K_2 second high-vacuum tap. K_4-K_6 grease cocks. M_2 Pirani (hot-wire) gauge. R_2 reservoir containing carbon monoxide. *V* expansion volume of 5.2 l. *C* liquid-nitrogen trap. L_1 capillary. The mercury diffusion pump is connected to *P*. The control valve K_3 and methane-filled bulb R_1 can be connected to point *A*.

---

[6] R. H. Collins and J. C. Turnbull, Vacuum **10**, 27, 1960 (No. 1/2).

easily be achieved. The residual gas is then primarily nitrogen. The lower pressure must therefore be attributed entirely to the absence of gas given off by the epoxy resin. Provided the pressure in the picture tube is much higher than 5×10^{-8} torr, which is always the case in practice, this method is therefore permissible.

Reasonable agreement is found between the composition of the residual gases in the picture tube before it is broken open (measured with a second omegatron fixed directly to the bulb) and the composition found after the tube is broken open. The only difference found after breaking open the tube is that the pressures of the water vapour and carbon dioxide are lower, owing to absorption on the well-degassed components of the pump system.

Fig. 10 shows the composition of the residual gases in two picture tubes that were rejected on the grounds of excessive gas pressure and were broken open in the manner described. These tubes were found to contain hydrocarbons, water vapour and argon. The hydrocarbons were probably due to reactions between water vapour and carbon compounds in the getter film [7]). In other picture tubes the excessive pressure was sometimes found to be attributable to argon. The latter tubes showed no leakage, as was proved by storing them for a considerable period in plastic envelopes filled with helium. At the end of this time the omegatron registered no higher helium pressure. It is probable that air entered these tubes *during the pumping process*. The active gases would then be taken up by the getter film, but not the inert gas argon.

The remainder of the system represented in fig. 9 serves for investigating the gettering capacity of the barium getter in the picture tube [8]). For this measurement K_2 is closed and K_1 opened. The carbon monoxide is admitted from a bulb having a known volume V of 5.2 l. The pressure p_2 in V is measured with a Pirani (hot-wire) gauge, which is specially calibrated for carbon monoxide. In this way a known quantity of gas can be admitted to the getter film. The pumping speed S of the getter can be found from the equation

$$S = L \frac{p_2 - p_1}{p_1}, \quad \ldots \ldots \quad (7)$$

where p_1 is the carbon-monoxide pressure in the picture tube and L the conductance between the bulb and the picture tube. The conductance is almost entirely determined by the capillary L_1. The pressure p_1 in the picture tube can be measured by using the electron gun of the tube itself as an ionization gauge [9]). The procedure is illustrated in *fig. 11.*

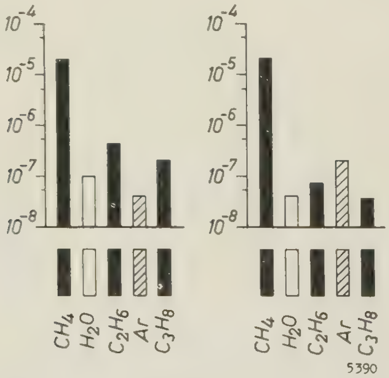

Fig. 10. Composition of residual gases in two picture tubes from normal production, rejected because of their excessive gas pressure.

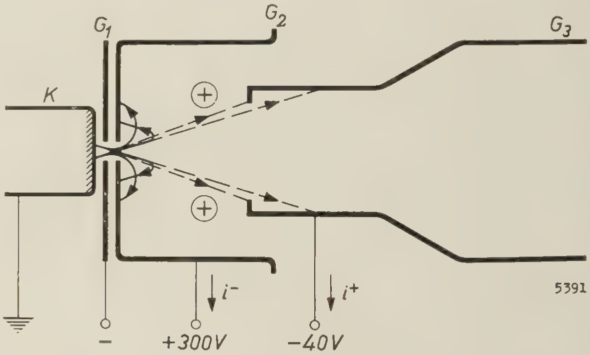

Fig. 11. Pressure measurement in a picture tube using the electron gun itself as an ionization gauge. K cathode at earth potential. G_1 grid negative to earth. G_2 positive grid which collects the electrons. The ion current, which is a measure of the pressure, is measured with G_3.

The cathode is kept at earth potential. With the aid of the first negative grid the electron beam is directed on to the second grid, which has a potential of 300 V positive to the cathode. All other electrodes are given a potential of 40 V negative to the cathode. These electrodes are used to determine the ion current, which in this case is a measure of the pressure.

The total amount of carbon monoxide that a getter film in a picture tube can take up depends on the evaporated quantity of getter material. A representative value is 1 torr-litre when 45 mg of barium is evaporated in a 21″ picture tube.

Other kinds of electron tubes that can be broken open and analysed in this way are oscilloscope tubes, transmitting tubes and television pick-up tubes, such as vidicons and image orthicons. Generally speaking it can be said that any electron tube can be investigated in this way, provided the quantity of gas in the tube is greater than 10^{-7} torr l.

---

[7]) F. H. R. Almer, H. J. R. Perdijk and P. G. van Zanten, Advances in vacuum science and technology, Proc. 1st int. congress on vacuum techniques, Namur, 10th-13th June 1958, Part 2, p. 676, Pergamon Press, Oxford 1960.

[8]) J. J. B. Fransen and H. J. R. Perdijk, Philips tech. Rev. **19**, 290. 1957/58.

[9]) J. de Gier, Ingenieur **65**, O 36, 1953.

An example of the analyses of an image orthicon can be seen in *fig. 12.* In this case the residual gases were analysed four months after manufacttre, and were found to consist of methane, ethane and argon from the barium getter. Also found was a partial pressure of 2×10^{-6} torr for helium, which had diffused through the glass wall from the outside atmosphere. The quantity Q of helium that diffuses per unit time through a surface of area A and thickness d, at a pressure difference across the wall Δp, is given by:

$$Q = \frac{KA\Delta p}{d} \quad . \quad . \quad . \quad . \quad . \quad . \quad (8)$$

Here K is the permeability of helium of the borosilicate glass used, given by 10)):

$$K = 1.5 \times 10^{-13} \frac{\text{torr-litre} \times \text{mm (thickness glass wall)}}{\text{cm}^2 \text{ (surface)} \times \text{sec} \times \text{torr (He pressure diff.)}}\,.$$

In the case of the image orthicon, A was 600 cm^2, Δp was 3×10^{-3} torr, and the average wall thickness d 2.2 mm. The volume of the orthicon was 740 cm^3, giving a calculated pressure rise after four months of 1.9×10^{-6} torr. This is in excellent agreement with the measured helium pressure of 2×10^{-6} torr.

Decomposition of hydrocarbons in a picture tube during operation

When the electron gun of a picture tube is used as an ionization gauge in the manner described above, the partial pressures of the hydrocarbons measured with the omegatron are found to decrease very rapidly. This is due to the disintegration of hydrocarbons on the hot cathode, which is at a temperature of 800 °C, and to the subsequent uptake of the fragments in the getter film. Furthermore, the collision of electrons with gas molecules gives rise to ions which are captured by the negative electrodes. Both mechanisms contribute to the reduced partial pressures of the hydrocarbons. A plot of the decrease measured in a picture tube is shown in *fig. 13.* The heavier hydrocarbon molecules decompose more rapidly than the light ones, so that the partial pressures of the heavier molecules decrease faster than that of methane molecules, for example, which are light. The pumping speed for the latter can be found from the formula:

$$V \frac{\mathrm{d}p}{\mathrm{d}t} = -Sp\,, \quad . \quad . \quad . \quad . \quad . \quad . \quad (9)$$

where V is the volume, p the pressure, $\mathrm{d}p/\mathrm{d}t$ the pressure change per unit time and S the pumping speed. After integration we find:

$$\ln \frac{p}{p_0} = -\frac{S}{V}t, \quad . \quad . \quad . \quad . \quad . \quad . \quad (10)$$

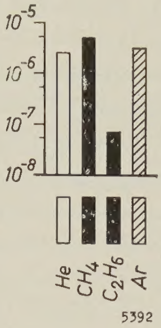

Fig. 12. Composition of the residual gases in an image orthicon four months after manufacture. Note the high helium pressure.

where p_0 is the pressure at $t = 0$. The pumping speed can thus be found from the slope of the curve obtained by plotting the logarithm of the pressure against time. The pumping speed found in this way for methane is roughly 0.004 l/sec.

The pumping speed for hydrocarbons is much higher during normal operation of the tube, when a screen is bombarded by electrons of energy 16 keV. The exceptionally high pumping speed cannot be explained by the longer path of the electrons through the tube and the consequent larger number of ions formed. The production of ions does not even increase linearly with the length of the electron

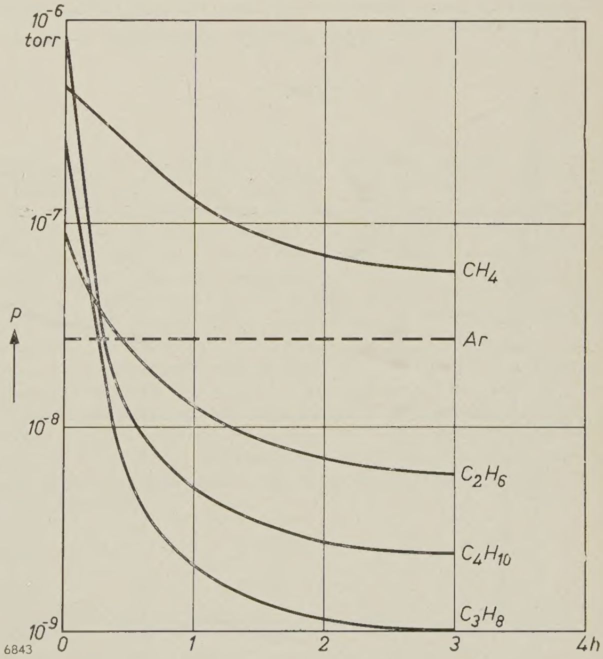

Fig. 13. Decrease in the partial pressure of hydrocarbons in a picture tube. The logarithm of the pressure is plotted versus time in hours. Electron current 400 μA. The electron gun of the tube was used as an ionization gauge.

---

10) A. Klopfer and W. Ermrich, Vacuum **10**, 128, 1960 (No. 1/2).

trajectories, since the electrons now have a higher energy and therefore their ionization probability is less than when the electron gun is used as an ionization gauge. The conclusion, then, is that the high pumping speed for hydrocarbons is attributable to the *fluorescent screen*. This is clearly demonstrated in *fig. 14*, where the logarithm of the methane pressure is plotted as a function of time from the beginning of the screen bombardment. Curve 1 relates to a finished picture tube, and curve 2 to a tube without a fluorescent screen but containing the conductive aluminium coating. In the latter tube the pumping speed for methane is again 0.004 l/sec, compared with 2 l/sec in the finished tube. A similar comparison of two tubes, one of which had a silicate binder added to the fluorescent screen and the other not, revealed that the silicate binder is responsible for the high pumping speed for hydrocarbons. The form in which the silicate binder is present after preparation of the screen shows much resemblance to silica gel, a substance possessing a large internal surface and capable of adsorbing large amounts of gas.

The fact that the fluorescent screen is responsible for the pumping effect is again clearly apparent from the effect of the accelerating voltage. The effect is not perceptible until 1.5 kV, i.e. the same potential at which the electrons are able to penetrate through the aluminium layer to the phosphor coating. Up to 4 kV the pumping speed continues to rise, and above this value it is independent of the voltage.

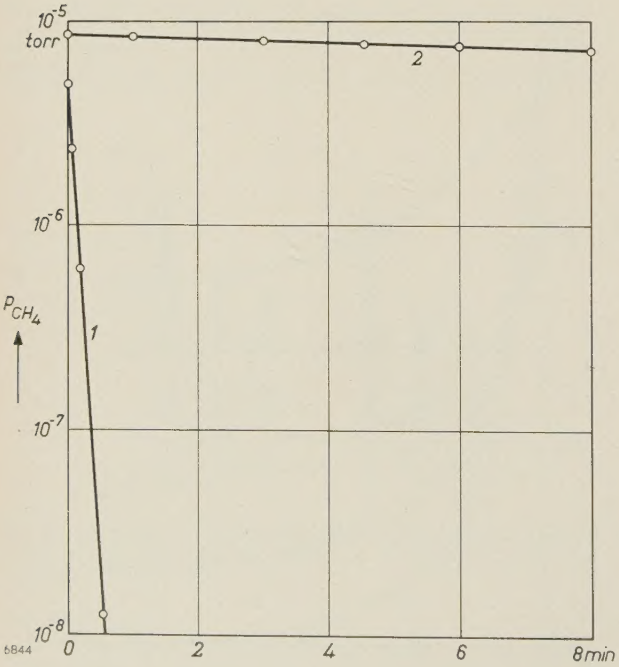

Fig. 14. Adsorption of methane during bombardment of the screen in a finished picture tube (*1*) and in a tube without fluorescent screen (*2*). Constant pumping speeds are inferred from the slopes of the two curves.

Various experiments were done to investigate the mechanism of this pumping effect. A finished picture tube was connected by a glass tube to the pumping system shown in fig. 9. The connecting tube was temporarily closed off by a thin-walled glass bulb. The bulb R_1, filled with methane, was connected to the pump system at A via a control valve K_3. The part of the system shown within dotted lines in the figure was degassed for 15 hours at 400 °C. The picture tube was kept at room temperature. At the end of this period the total pressure measured with the omegatron was roughly 10^{-8} torr. The residual gases consisted almost entirely of hydrogen, nitrogen and carbon dioxide. Communication with the picture tube was then established by breaking the thin-walled bulb with a steel ball. The high-vacuum valve K_1 was closed, after which the picture tube was given a methane pressure of about 5×10^{-6} torr by adjustment of the control valve K_3. The omegatron was adjusted so as to bring ions having a mass 16 into resonance, making it possible to determine the methane pressure continuously throughout the experiment. During this time the electron beam scanned a variable area on the fluorescent screen. *Fig. 15* shows the logarithm of the methane pressure plotted versus time from the moment of switching on the tube, for five different scanning areas. The current density of the electron beam at the screen was at all times 1 μA/cm^2, the accelerating voltage 16 kV. Whether the barium getter was evaporated or not had no effect on the results.

Similar experimental runs were carried out for different current densities at the screen. They all gave results resembling those in fig. 15, except that the pressure decreased more rapidly the higher the current density.

The characteristic shape of the curves in fig. 15 may be explained qualitatively as follows. We suppose that the electrons, in bombarding the screen, give rise to active centres in the silicate binder of the fluorescent coating, as a result of which the incident methane molecules are trapped and at the same time hydrogen is desorbed. During the initial bombardment of the screen the number of centres increases and so does the pumping speed. Assuming that the number of centres reaches a maximum after a certain time, it follows that the pumping speed must then become constant. This is the case in the linear portion of the curve in fig. 15. After some considerable time a state of equilibrium is

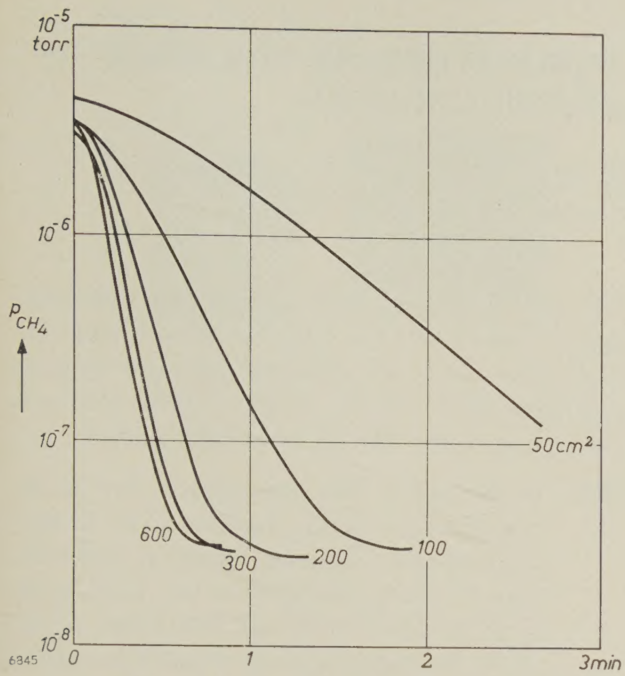

Fig. 15. Variation of methane pressure in a picture tube. The logarithm of the pressure is plotted as a function of time in minutes for five different values of the scanned area. The current density of the electron beam was kept constant ($j = 1$ μA/cm² on the screen). $V_a = 16$ kV.

reached in which the pressure remains constant. In this state the adsorption of methane is equal to its desorption.

The mechanism may be described in somewhat greater detail as follows. Let n_0 be the maximum number of centres formed per unit area and N the number of centres already produced on the scanned area A. The number of centres that can still be produced is then $An_0—N$. Experiment shows that the rate of change of $An_0—N$ is proportional to the current density j at the screen. It is also found that the active centres have a certain lifetime and that the number vanishing per unit time is proportional to the number present. The number of centres that disappear as a result of methane adsorption is negligibly small. The number of centres appearing or vanishing per unit time is therefore given by:

$$\frac{dN}{dt} = k_1 j (An_0 - N) - k_2 N. \quad . \; . \; . \quad (11)$$

where k_1 and k_2 are constants. At equilibrium we have:

$$\frac{dN}{dt} = 0 \, , \quad . \; . \; . \; . \; . \; . \; . \; . \; . \quad (12)$$

and therefore, putting $k_1/k_2 = k$, we find:

$$N = \frac{k_1 j A n_0}{k_1 j + k_2} = \frac{kjAn_0}{kj+1} \, . \quad . \; . \; . \; . \; . \quad (13)$$

The number of methane molecules adsorbed by the screen per unit time, i.e. $V\,dp/dt$, is proportional to the number of active centres and to the pressure:

$$V \frac{dp}{dt} = -aNp \, , \quad . \; . \; . \; . \; . \; . \; . \quad (14)$$

where a is a proportionality factor. Combining this expression with equation (9) it follows that the pumping speed S is equal to $+aN$, or, denoting the maximum pumping speed per unit area, an_0, by s_0:

$$S = \frac{kjAs_0}{kj + 1} \, . \quad . \; . \; . \; . \; . \; . \; . \; . \; . \quad (15)$$

In the linear portion of the "characteristic" in fig. 15 the pumping speed is constant and the number of centres formed under the given conditions is maximum. The maximum pumping speed per cm² is $s_0 = 0.01$ l/sec, and the constant $k = 2.0$. The formula derived shows good agreement with the experimental values of the pumping speed found for different values of scanned area A and current density j at the screen. The formula is valid up to a scanned area of 300 cm², above which the increase in pumping speed is less than follows from the formula.

The high pumping speed for methane in a picture tube during operation considerably reduces the partial pressure of the methane. A finished picture tube, when not in operation, often contains more methane than any other gas. This is due to the fact that methane may be produced at room temperature by reactions between water vapour and carbon in the getter film. There is no uptake of methane in the barium getter itself. If the methane were not to disappear during operation, the ionic bombardment of the cathode would be very much stronger and the life of the tube would therefore be shortened. This illustrates clearly how important it is to know the composition of the residual gases and to investigate the various processes that may take place inside a television picture tube.

Summary. In the manufacture of television picture tubes it is important to know not only the total pressure in the tubes but also the composition of the residual gases. This information can readily be obtained with an omegatron. After briefly describing the principle of the omegatron for quantitative analyses and the experimental system used, the authors discuss the desorption of gas by various parts of the picture tube. A method of analysing the composition of the gas in sealed-off tubes is described and some results are given. Finally, experiments are discussed which demonstrate the high uptake of methane by the fluorescent screen in a picture tube during electron bombardment. This removal of desorbed methane takes place continuously during the normal operation of a picture tube. It is attributable to the silicate binder used in the screen, and it guards the cathode against damage by ion bombardment.

ABSTRACTS OF RECENT SCIENTIFIC PUBLICATIONS BY THE STAFF OF N.V. PHILIPS' GLOEILAMPENFABRIEKEN

Reprints of these papers not marked with an asterisk * can be obtained free of charge upon application to Philips Electrical Ltd., Century House, Shaftesbury Ave., London W.C. 2, where a limited number of reprints are available for distribution.

2865: F. N. Hooge: Relation between electronegativity and energy bandgap (Z. phys. Chemie Neue Folge (Frankfurt a.M.) **24**, 275-282, 1960, No. 3/4).

It is shown that there exists a relation between the energy gap of crystals with formula AB and the electronegativities of the atoms A and B. The values of the electronegativities are the only quantities needed for the estimation of the width of the energy gap.

2866: G. Thirup: The application of phase-locking techniques to the design of apparatus for measuring complex transfer functions (J. Brit. Instn. Radio Engrs. **20**, 387-396, 1960, No. 5).

The theory of phase-lock synchronization is given briefly. Two devices for measuring complex voltage ratios are described. In the first, which has a frequency range 1-110 Mc/s, the voltage ratio to be measured is converted to a constant intermediate frequency of 450 kc/s. The frequency difference between the signal generator and the local oscillator is kept constant by coupling the tuning shafts mechanically and by a phase-lock synchronizing device; special means for extending the pull-in range, making use of a coarse and fine electronic adjustment, are described. The second instrument has a frequency range of 30-700 Mc/s, and here the local and signal generators are free-running and are separately tuned manually. A double frequency conversion system is used. The frequency of the second local oscillator, by means of a phase-lock device, is kept 450 kc/s below the frequency difference of the signal and first local oscillator. A description is also given of how the complex measuring results can be displayed on a cathode-ray tube.

2867: M. Avinor: Gold-activated (Zn,Cd)S phosphors (J. Electrochem. Soc. **107**, 608-611, 1960, No. 7).

Gold is shown to produce three emission bands in CdS, at 640, 800 and 1150 mμ. The long-wave band appears only when a coactivator is used, while the short-wave bands are observed with activation by gold alone. The 1150 mμ band in CdS is shown to correspond to the 530 mμ gold band in ZnS.

2868: H. Bremmer: The propagation over an inhomogeneous earth considered as a two-dimensional scattering problem (Electromagnetic wave propagation, int. Conf. sponsored by the Postal and Telecomm. Group of the Brussels Universal Exhibition, edited by M. Désirant and J. L. Michiels, pp. 253-260, Academic Press, London 1960).

This article deals with a two-dimensional integral equation for the distribution of field strength across a flat inhomogeneous earth. The equation in question is based on an approximative boundary condition, which accounts for the local distribution of the electrical constants. An infinite series representing the solution is interpreted in terms of scattering effects. The result applying to a special situation (two homogeneous regions separated by a straight boundary) is compared with that derived from the conventional one-dimensional equation which constitutes a saddlepoint approximation of the above two-dimensional equation.

2869: C. Z. van Doorn and Y. Haven: Anisotrope kleurcentra in KCl (Ned. T. Natuurk. **26**, 216-220, 1960, No. 7). (Anisotropic colour centres in KCl; in Dutch.)

When a KCl crystal is coloured by heating in K vapour (F absorption band at 5340 Å) and then irradiated at room temperature with light absorbed in the F band, a new (M) band appears at 8080 Å. After irradiation at 77 °K with polarized light absorbed in the F band, both the F and M bands are found to be dichroic. The authors interpret this effect by assuming the M band to be caused by two neighbouring F centres. The merits of this model are compared with those of similar models proposed by Seitz and by Knox.